

ornl

ORNL/TM-13566

RECEIVED

APR 08 1998

OSTI

**OAK RIDGE
NATIONAL
LABORATORY**

LOCKHEED MARTIN



**Homogeneous Reactor
Experiment (HRE) Pond
Cryogenic Barrier Technology
Demonstration: Pre-Barrier
Subsurface Hydrology and
Contaminant Transport
Investigation**

Gerilynn R. Moline

MANAGED AND OPERATED BY
LOCKHEED MARTIN ENERGY RESEARCH CORPORATION
FOR THE UNITED STATES
DEPARTMENT OF ENERGY

ORNL-27 (3-96)

This report has been reproduced directly from the best available copy.

Available to DOE and DOE contractors from the Office of Scientific and Technical Information, P.O. Box 62, Oak Ridge, TN 37831; prices available from (615) 576-8401, FTS 626-8401.

Available to the public from the National Technical Information Service, U.S. Department of Commerce, 5285 Port Royal Rd., Springfield, VA 22161.

This report was prepared as an account of work sponsored by an agency of the United States Government. Neither the United States Government nor any agency thereof, nor any of their employees, makes any warranty, express or implied, or assumes any legal liability or responsibility for the accuracy, completeness, or usefulness of any information, apparatus, product, or process disclosed, or represents that its use would not infringe privately owned rights. Reference herein to any specific commercial product, process, or service by trade name, trademark, manufacturer, or otherwise, does not necessarily constitute or imply its endorsement, recommendation, or favoring by the United States Government or any agency thereof. The views and opinions of authors expressed herein do not necessarily state or reflect those of the United States Government or any agency thereof.

**Homogeneous Reactor Experiment (HRE) Pond Cryogenic Barrier Technology
Demonstration: Pre-Barrier Subsurface Hydrology and
Contaminant Transport Investigation**

Gerilynn R. Moline
Environmental Sciences Division
Oak Ridge National Laboratory

March, 1998

Prepared by
Environmental Sciences Division
Oak Ridge National Laboratory
ESD Publication 4732

Prepared for
U.S. Department of Energy
Office of Environmental Restoration and Waste Management
under budget and reporting code EW 40 10 00 0

OAK RIDGE NATIONAL LABORATORY
Oak Ridge, Tennessee 37831-6285
managed by
LOCKHEED MARTIN ENERGY RESEARCH CORPORATION
for the U.S. Department of Energy
under contract number DE-AC05-96OR22464

MASTER

DISTRIBUTION OF THIS DOCUMENT IS UNLIMITED

DISCLAIMER

Portions of this document may be illegible electronic image products. Images are produced from the best available original document.

CONTENTS

FIGURES	ii
TABLES	iii
EXECUTIVE SUMMARY	iv
1. INTRODUCTION	1
1.1. BACKGROUND	1
1.2. SOIL CHARACTERIZATION	4
1.3. SITE GEOLOGY	14
1.4. ELECTROMAGNETIC GEOPHYSICAL SURVEY	14
2. HYDROLOGIC INVESTIGATION METHODS	16
2.1. SITE INSTRUMENTATION	16
2.2. TRACER TESTING	16
2.3. PIEZOMETRIC MONITORING	19
2.4. DRILLING LOGS AND GEOLOGIC RECONSTRUCTION	19
3. HRE-POND HYDROLOGY	19
3.1. WATER TABLE CONFIGURATION	19
3.2. STORM RESPONSE	22
3.3. HYDRAULIC CONDUCTIVITY	35
4. CONTAMINANT TRANSPORT PATHWAYS	35
4.1. HELIUM AND DYE TRACER DISTRIBUTION	35
4.2. SOIL CONTAMINATION PATTERNS	36
4.3. HRE-POND GEOLOGIC CROSS SECTIONS	42
5. CONCLUSIONS	49
5.1. CONCLUSIONS	49
5.2. RECOMMENDATIONS	49
6. REFERENCES CITED	51

FIGURES

Figure:

1. Site location map.	2
2. HRE-Pond construction diagram.	3
3. 1951 aerial photograph.	5
4. 1956 aerial photograph.	6
5. 1961 aerial photograph.	7
6. 1967 aerial photograph.	8
7. 1969 aerial photograph.	9
8. 1971 aerial photograph.	10
9. 1973 aerial photograph.	11
10. 1981 aerial photograph.	12
11. 1984 aerial photograph.	13
12. EM-31 survey grid and interpretation.	15
13. Well and standpipe locations.	17
14. Water table map.	21
15. Manual water levels in the standpipes.	23
16. Manual water levels in the wells.	24
17. S-2 hydrograph.	25
18. S-3 hydrograph.	26
19. S-5 hydrograph.	27
20. S-6 hydrograph.	28
21. S-8 hydrograph.	29

22. S-10 hydrograph.	30
23. I-2 hydrograph.	31
24. Well 1110 hydrograph.	32
25. Well 0673 hydrograph.	33
26. Well 0898 hydrograph.	34
27. Helium tracer distribution.	38
28. Aerial distribution of contaminated soils.	40
29. Cross sections showing the original drainage configuration.	41
30. West wall geologic cross section.	43
31. North wall geologic cross section.	45
32. East wall geologic cross section.	46
33. South wall geologic cross section.	47
34. South end geologic cross section.	48

TABLES

Table:

1. Well construction information.	18
2. Manual water level data.	20
3. Summary of helium tracer detects.	37

EXECUTIVE SUMMARY

The Homogeneous Reactor Experiment (HRE) Pond is the site of a former impoundment for radioactive wastes that has since been drained, filled with soil, and covered with an asphalt cap. The site is bordered to the east and south by a tributary that empties into Melton Branch Creek and that contains significant concentrations of radioactive contaminants, primarily ^{90}Sr . Because of the proximity of the tributary to the HRE disposal site and the probable flow of groundwater from the site to the tributary, it is hypothesized that the HRE Pond is a source of contamination to the creek. As a means for temporary containment of contaminants within the impoundment, a cryogenic barrier technology demonstration was initiated in FY96 with a background hydrologic investigation that continued through FY97. Cryogenic equipment installation was completed in FY97, and freezing was initiated in September of 1997.

This report documents the results of a hydrologic and geologic investigation of the HRE Pond/cryogenic barrier site. The purpose of this investigation is to evaluate the hydrologic conditions within and around the impoundment in order to meet the following objectives: 1) to provide a pre-barrier subsurface hydrologic baseline for post-barrier performance assessment; 2) to confirm that the impoundment is hydraulically connected to the surrounding sediments, and 3) to determine the likely contaminant exit pathways from the impoundment. The methods of investigation included water level and temperature monitoring in a network of wells and standpipes in and surrounding the impoundment, a helium tracer test conducted under ambient flow conditions, and geologic logging during the drilling of boreholes for installation of cryogenic probes and temperature monitoring wells.

Manual water levels obtained during the summer of FY96 indicated a very dynamic hydrologic setting both within and surrounding the impoundment, and suggested the potential for episodic transport of contaminants via a gravel layer located immediately below the asphalt cap in association with rain events. Subsequent continuous water level and temperature logging confirmed the rapid response to rain events including water levels in the standpipe located within the impoundment. A helium tracer test initiated in the summer of FY96 under ambient flow conditions initially resulted in very little detection of helium outside of the impoundment. However, a second injection during the wet winter months of FY97 resulted in helium transport to many locations in a radial pattern surrounding the impoundment. The two data sets combined demonstrated that the impoundment is not hydrologically isolated from the surrounding sediments and that transport out of the impoundment does occur, particularly under high water conditions. Geologic cross sections were constructed along each wall of the cryogenic barrier and included the locations of highest soil contamination. These cross sections combined with subsurface water level and temperature data and impoundment and cap construction information point to probable exit pathways and contaminant release mechanisms at a variety of depths.

This study concludes that contaminant transport is exacerbated by storm events, as previously discussed, and that multiple exit pathways exist and are controlled by the preexisting geology, the construction design of the impoundment, and the design of the asphalt cap. These potential

pathways include 1) transport from the base of the pond through the highly fractured shallow bedrock, possibly enhanced by the sand-filled boreholes that provide vertical pathways through the pond sediments, and through the fill around the effluent pipeline; 2) transport through the more permeable fill materials overlying the original impoundment; 3) transport through the gravel layer immediately below the asphalt cap; and 4) transport through the walls of the original impoundment, possibly related to influent/effluent pipelines and fractures in the walls of the pond. This study also concludes that differences in transport of the dye and gas tracers is most likely due to flooding the impoundment for several days following dye injection.

The following actions are recommended to provide independent verification of the performance of the cryogenic barrier:

1. *Post-barrier tracer tests using bromide and a continuous injection method similar to that used at WAG 5.* Continuous injection allows sufficient mass to be introduced over time, avoids artificially raising the water table in the pond, and avoids density effects. Bromide is inexpensive, non-sorbing, can be easily analyzed with ion chromatography methods for sensitive detection, and circumvents any uncertainty associated with previous dye injections at this and surrounding sites.
2. *Designing sampling strategies for monitoring releases from the impoundment that take episodic transport into account.* Sampling for tracers and/or radionuclides must be conducted frequently enough and timed relative to storm events to capture any episodic transport behavior. Infrequent monitoring at pre-determined intervals may miss the transport of tracers unless sufficient mass is injected and sufficient time allowed to achieve consistent breakthrough.
3. *Continued water level and temperature monitoring throughout FY98.* Water level and temperature monitoring should be continued during and following the installation of the cryo-barrier in order to determine changes in subsurface hydrology related to barrier installation. Temperature monitoring can provide an indication of heat flux in the area surrounding the barrier. Continued monitoring through the year can be used to determine the impact of seasonal variations on barrier integrity.

1. INTRODUCTION

The Homogeneous Reactor Experiment (HRE) Pond is the site of a former impoundment for radioactive wastes that has since been drained, filled with soil, and covered with an asphalt cap. The site is bordered to the east and south by a tributary that empties into Melton Branch and that contains significant concentrations of radioactive contaminants, primarily ^{90}Sr . Because of the proximity of the tributary to the HRE disposal site and the probable flow of groundwater from the site to the tributary, it is hypothesized that the HRE Pond is a source of contamination to the creek.

The HRE-Pond was chosen as the site of a cryogenic barrier demonstration, to evaluate this technology as a means for rapid, temporary isolation of contaminants. A frozen wall is created by the circulation of liquid nitrogen through a system of thermoprobes installed at 6-foot intervals in 30-foot boreholes which are backfilled with sand. The probes cool the subsurface, creating a vertical ice wall by freezing adjacent groundwater, effectively surrounding the impoundment on all sides except the bottom.

The purpose of this investigation is to evaluate the hydrologic conditions within and around the impoundment. The objectives are 1) to evaluate the pre-barrier subsurface hydrology in order to provide a baseline for post-barrier performance assessment; and 2) to confirm that the impoundment is hydraulically connected to the surrounding sediments, and 3) to determine the likely contaminant exit pathways from the impoundment.

1.1. Background

The HRE Pond is located in Melton Valley immediately adjacent to several buildings that comprise the former experimental reactor complex (Figure 1). The impoundment was constructed in 1955 by excavating into the previous slope to create the northern and western sides of the pond, and by using earth fill to create the eastern and southern sides of the pond [Stansfield and Francis, 1986]. The maximum capacity of the impoundment was estimated at 310,000 gallons and was reportedly partially drained at one time to allow an asphalt coating to be sprayed on the upper portions of the impoundment walls. The lower portion of the pond was apparently unlined with the bottom of the pond at no more than a foot above bedrock, based on the results of soil cores obtained by augering through the impoundment [Stansfield and Francis, 1986].

While in operation from 1957-1962, the impoundment was used as a settling basin for low-level radioactive waste in the form of condensate from an evaporator in the process liquid waste system and shield water exposed to the reactor circuits. Contaminant settling was accelerated by the application of flocculants including ferric flocculants, trisodium phosphate, and diatomaceous earth. Figure 2 is an engineering drawing detailing the construction design for the impoundment, including the location of influent and effluent pipelines. Because these are not As-Built diagrams, it is not known how closely the actual construction matched the specifications shown in this drawing.

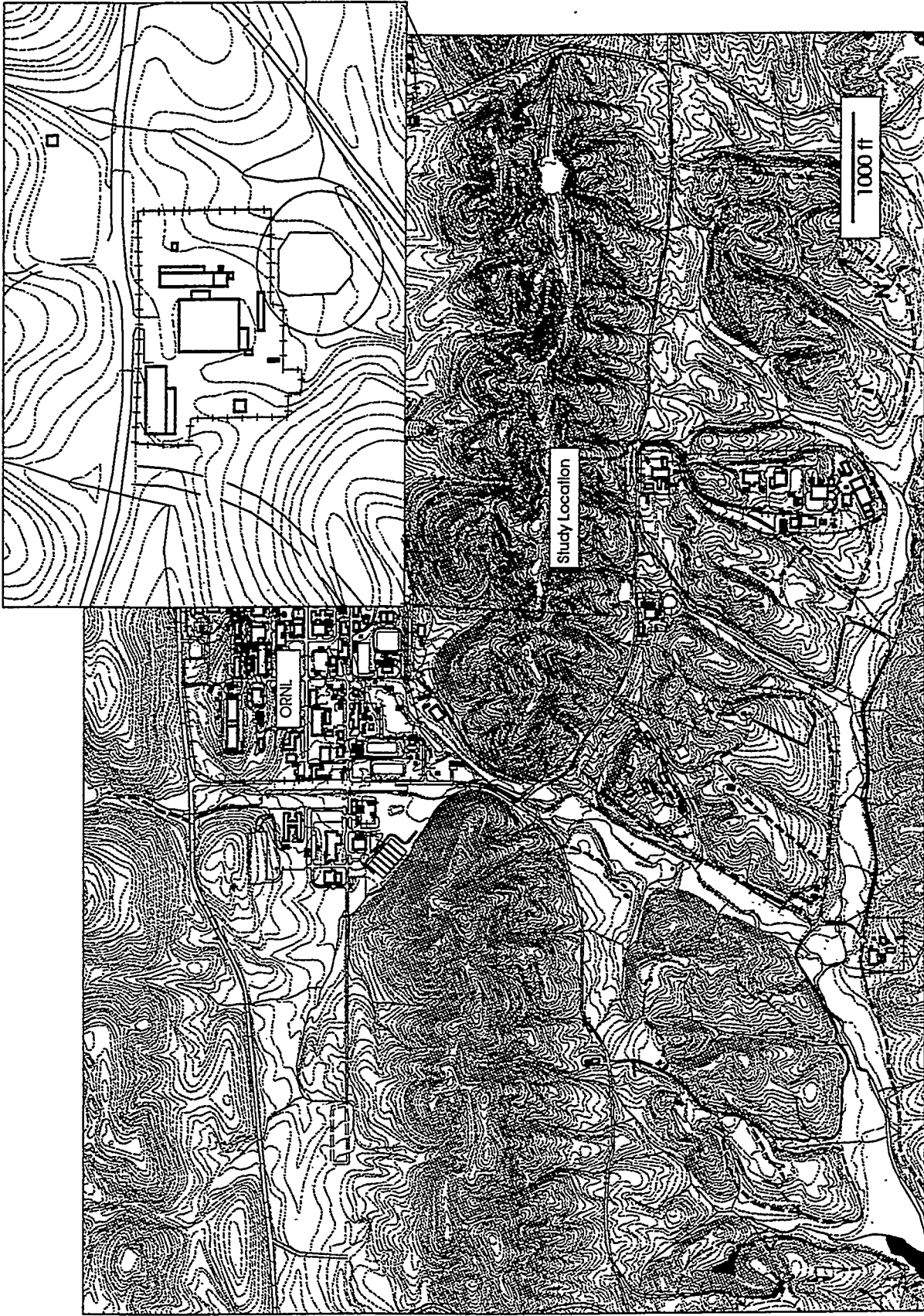


Figure 1: Site location near Oak Ridge National Laboratory (ORNL).

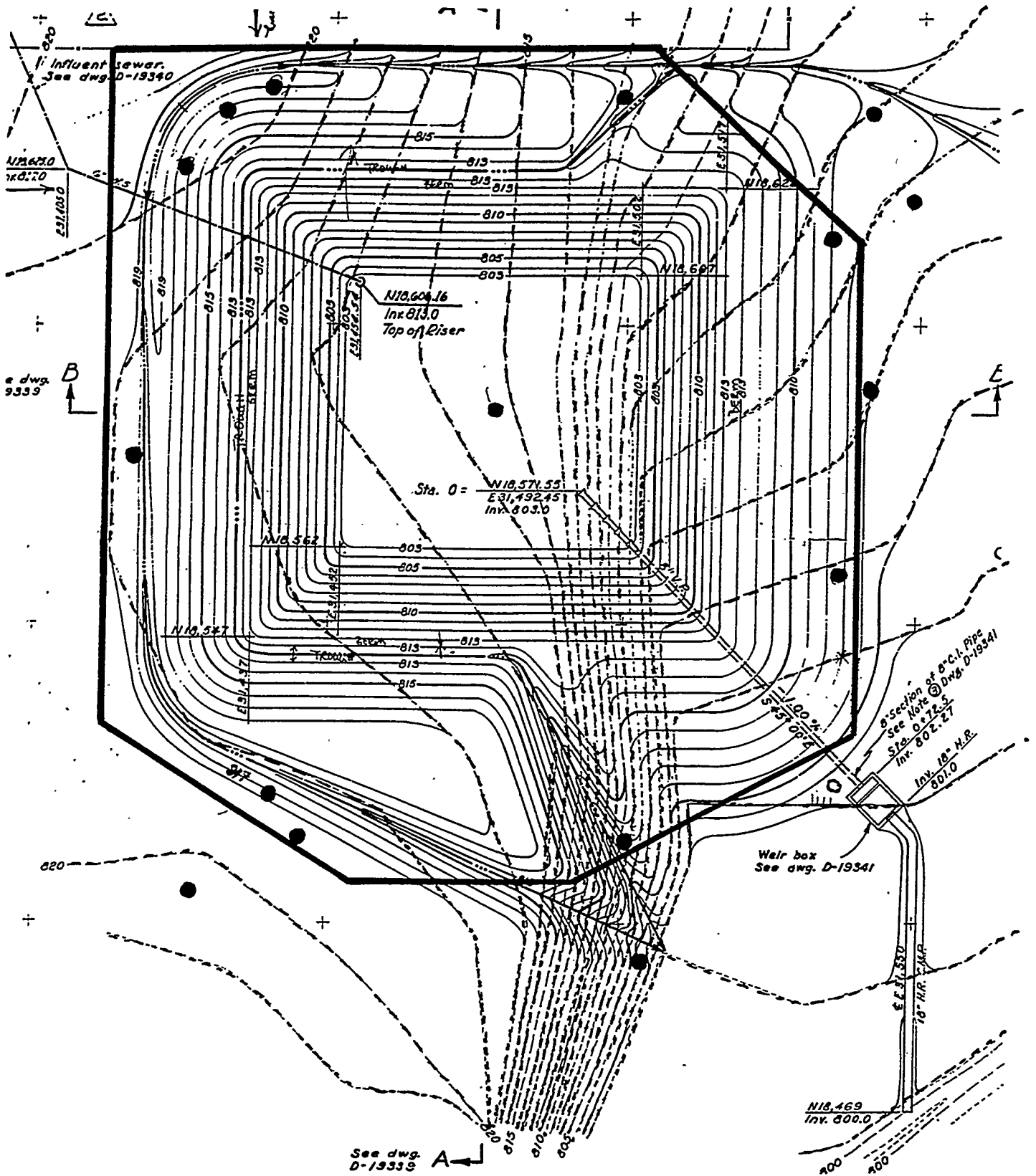


Figure 2. Engineering design for the HRE impoundment Dashed contours represent the original land surface before excavation. The boundary of the asphalt cap and well and standpipe locations have been added to the drawing. Note the location of the influent sewer line in the NW corner and the drainage pipeline in the SE corner. The original berm is located at 813' elevation.

In 1970, the pond was closed by filling with soils obtained from a source on the Oak Ridge Reservation (ORR). According to observers, the pond was approximately half full of water and sediments at the time of filling, and had accumulated between 1-2 feet of sediment at the bottom [Stansfield and Francis, 1986]. Following backfilling, the area was covered with a one- to two-foot layer of crushed limestone and capped with asphalt. Eight perforated steel drive point casings were then installed around the perimeter of the asphalt cap and one within the center of the impoundment. These standpipes were used as part of the monitoring network for this investigation.

A series of aerial photographs of Bethel and Melton Valleys obtained between 1951 and 1984 capture some of the changes in the region encompassing the HRE impoundment during its construction, use, and subsequent burial. Figures 3-11 contain enlargements of this region and are useful for estimating the footprint of the impoundment over time. However, the resolution is too coarse to be able to identify smaller features such as pipelines.

1.2. Soil characterization

In 1986, the soil and groundwater in and around the HRE impoundment was characterized in order to estimate the inventory of waste contained in the impoundment [Stansfield and Francis, 1986]. As part of these activities, six soil borings were obtained from within the impoundment and four monitoring wells were installed around the perimeter. Based on the soil tests, it was determined that ^{90}Sr and ^{137}Cs were the primary radiological constituents, with inventories estimated at 75 Ci and 16 Ci, respectively. Of interest to this investigation is the aborted drilling of a borehole located approximately two feet to the SW of 1112 (MW-4). Drilling at that location was terminated to prevent contaminated groundwater from being brought to the surface when radiation levels from the cuttings at a depth of 8.5 feet exceeded 1000 cpm ($\sim 0.3\text{mR/h}$) [Stansfield and Francis, 1986].

Detailed results of the soil analyses, found in the appendix of Stansfield and Francis [1986], are summarized here. Cores were obtained by advancing a split-spoon sampler ahead of the auger bit to a depth of refusal, which was described as highly fractured calcareous shale. In all cases, this depth exceeded the elevation of the base of the impoundment (803'). Boreholes were subsequently backfilled with sand and plugged with concrete at the surface. Similar soil patterns were encountered in each borehole: approximately four inches of asphalt, one foot of crushed limestone, brown clay fill mixed with shale and limestone fragments down to approximately five feet, followed by brown clayey soils with grey-colored zones and inclusions down to an elevation of 803 ft consistent with the bottom of the pond. The change in color from brown to mixed and the depth at which water was encountered in the soil cores coincided with the elevation of the top of the original impoundment (813 ft). The soil core located at the NW corner of the impoundment had the highest radiological levels, with a localized portion of the core reading approximately 100 mR at a depth consistent with the top of the pond.

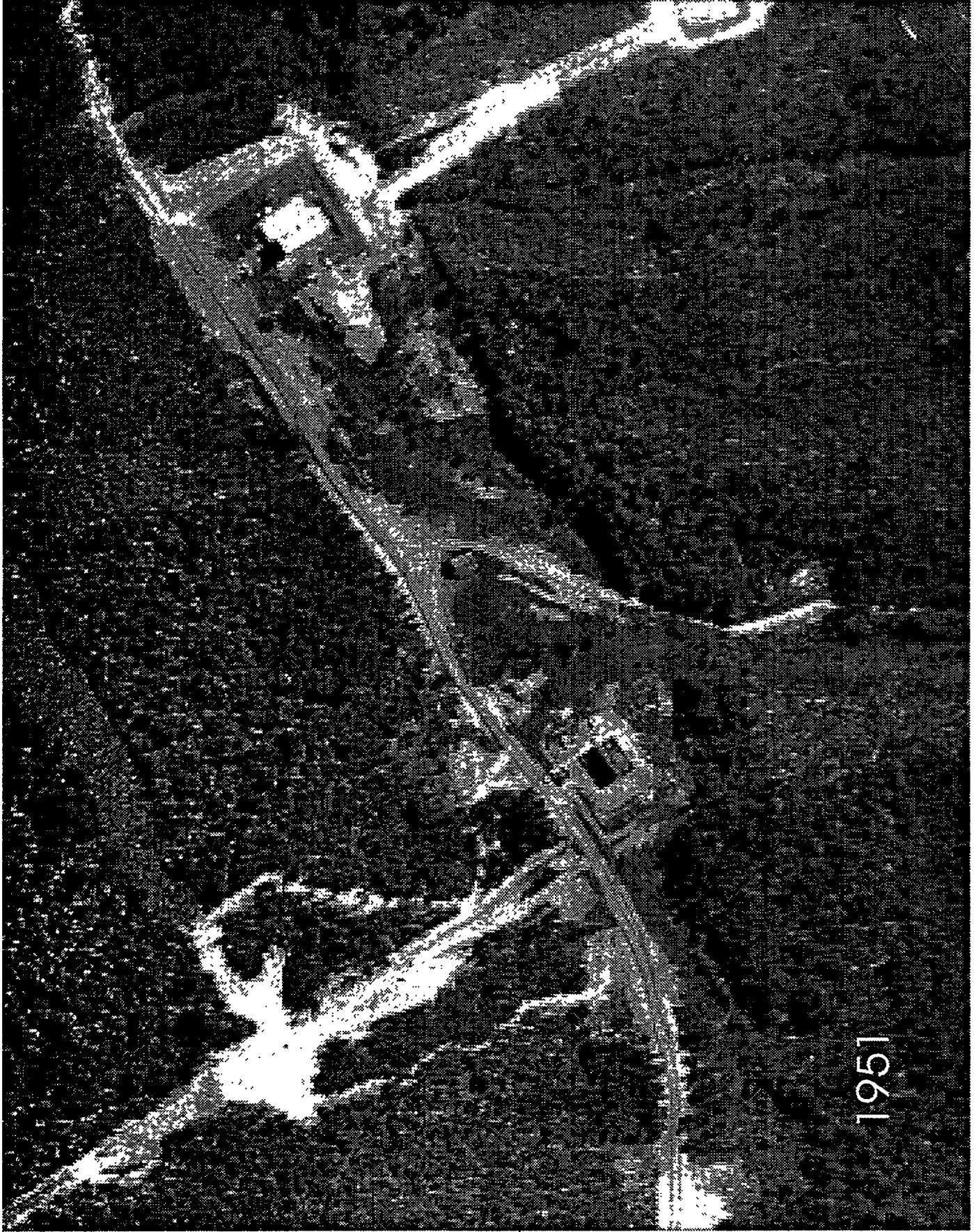


Figure 3. Air-photo of the HRE-Pond site during early construction.



Figure 4. Air photo of the HRE-Pond site during early excavation.



1961

Figure 5. Air photo of the HRE-Pond site during active use.



Figure 6. Air photo of the HRE-Pond site when no longer in use but before being capped.



Figure 7. Air photo of the HRE-Pond site while not in active use but before being capped.



Figure 8. Air photo of the Hre-Pond site immediately following closure.

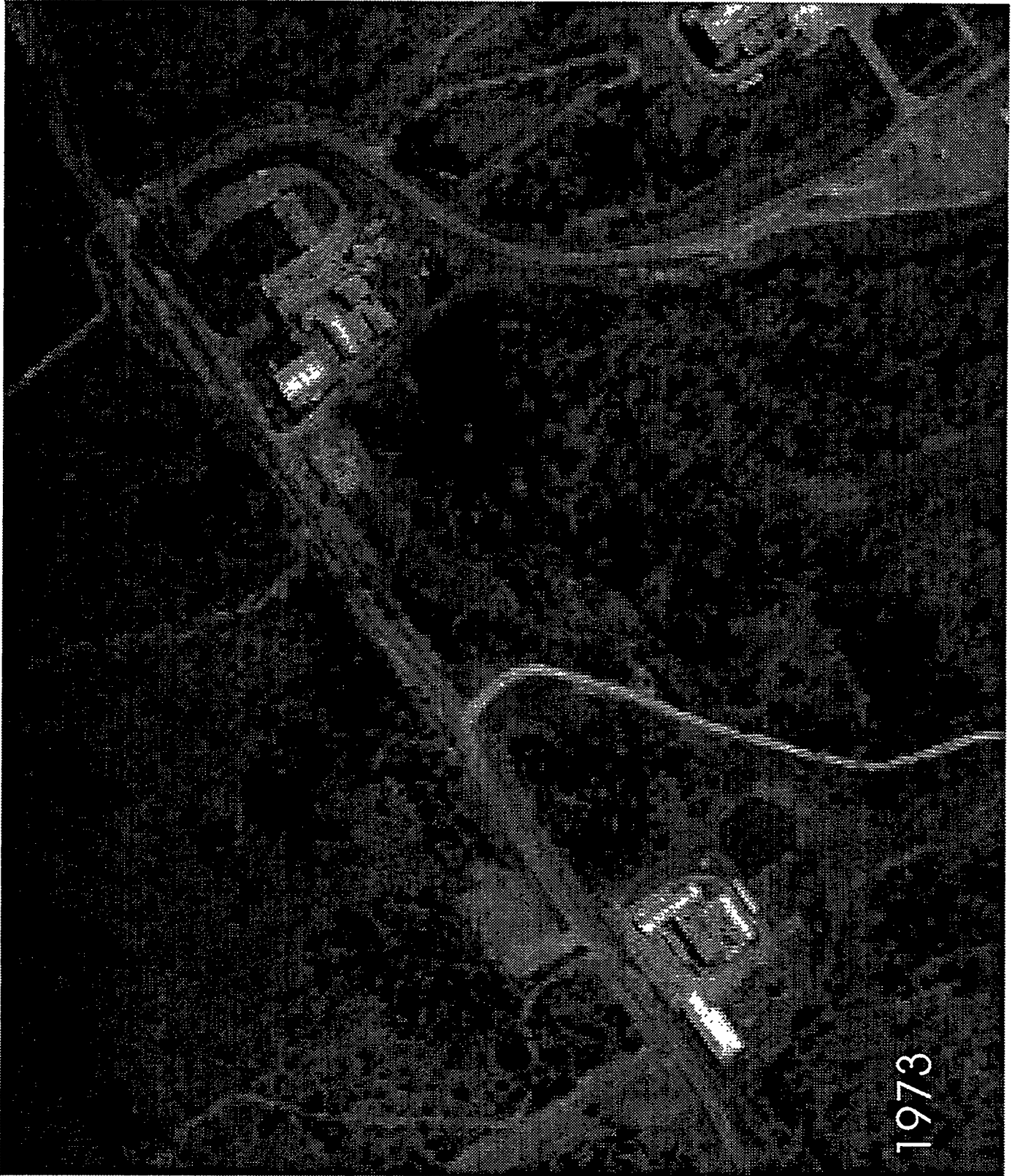
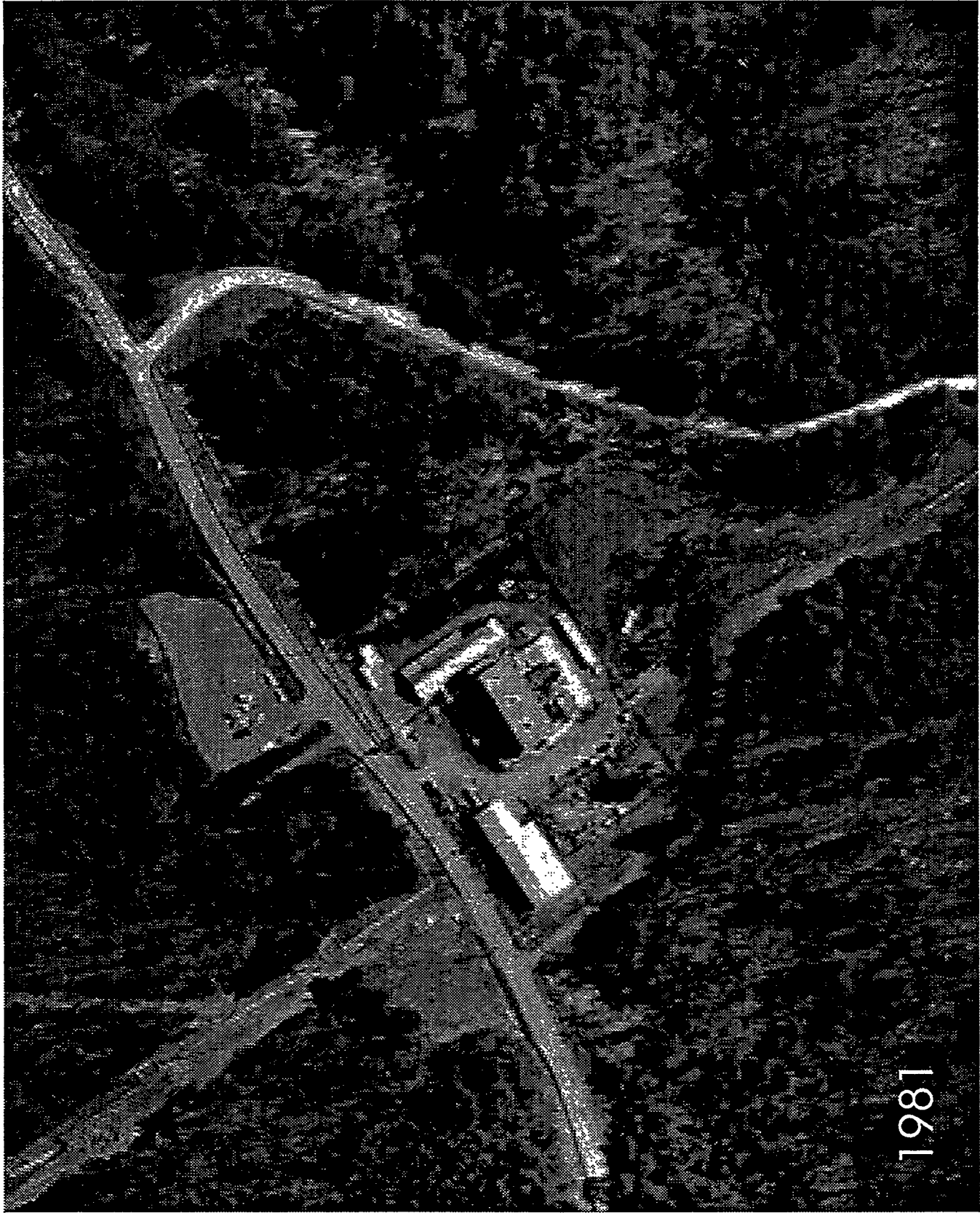


Figure 9. Air photo of the HRE-Pond site following closure.



1981

Figure 10. Air photo of the HRE-Pond site after closure.



Figure 11. Air photo of the HRE-Pond site after closure.

1.3. Site geology

Bedrock underlying the HRE-Pond area consists of two geologic units of the Conasauga Group: the Rogersville Shale and the underlying Friendship Formation (formerly Rutledge Limestone). The Rogersville Shale is characterized by interbedded maroon to chocolate-brown mudstones and grey to grey-green calcareous and noncalcareous siltstones. By contrast, the Friendship Formation consists of light-grey, micritic to coarsely crystalline thinly- to moderately-bedded limestone with dark grey or maroon shale interbeds (Hatcher et al., 1992). The contact between these geologic units is abrupt and marked by the absence of limestone beds and the appearance of maroon shale, and has been mapped at the surface ~ 20 ft. north of the asphalt cap. Locally, bedding dips from 30-40 degrees to the SE, making it likely that the deeper boreholes intersect the geologic contact at depth, particularly on the north end of the impoundment.

The bedrock is complexly fractured, and fractures and fracture intersections are likely to dominate groundwater flow and contaminant transport directions. Evidence of strike-preferential flow has been demonstrated through numerous tracer tests conducted in similar materials on the ORR as well as by contaminant distribution patterns. This phenomenon occurs irrespective of the direction of the hydraulic gradient.

Highly weathered shale saprolite forms a clay-rich cover over the undisturbed bedrock surrounding the impoundment. Because the saprolite retains the overall structure of the bedrock, including fractures, evidence of fracture-dominated flow is also seen in the shallow groundwater system within the saprolite elsewhere on the ORR. Weathering processes increase the porosity and clay content of the matrix material, resulting in low-permeability high porosity residuum that provides the means for significant storage of contaminants through matrix diffusion and sorption processes. Thus moderately to strongly sorbing solutes such as ^{90}Sr , ^{137}Cs , and some fluorescent dyes such as Rhodamine-WT are retained in the stagnant porewaters of the bedrock and saprolite where they can provide a secondary source over time.

1.4. Electromagnetic Geophysical Survey

In FY96 an electromagnetic conductivity survey of the HRE-Pond area was conducted to identify areas potentially containing buried drums, metallic pipes, and other metallic debris [Kaufmann, 1996]. The survey identified areas of high- and low-conductivity anomalies (Figure 12). One striking anomaly is the low-conductivity linear feature at the north end of the grid, extending through the north wall of the former impoundment and consistent with a subsurface pipe. Two other anomalies were interpreted as possible buried scrap metal in the NW and SE corners of the impoundment.

The in-phase components of the data are more sensitive to buried metallic objects, and the quadrature components are more related to the electrical conductivity of the ground which is controlled by clay content, moisture content, and groundwater conductivity [Kaufmann, 1996]. The quadrature data show generally much higher conductivity of the soils on the northern portion of the grid, identified as the high conductivity plume in Figure 12.

Figure 12.

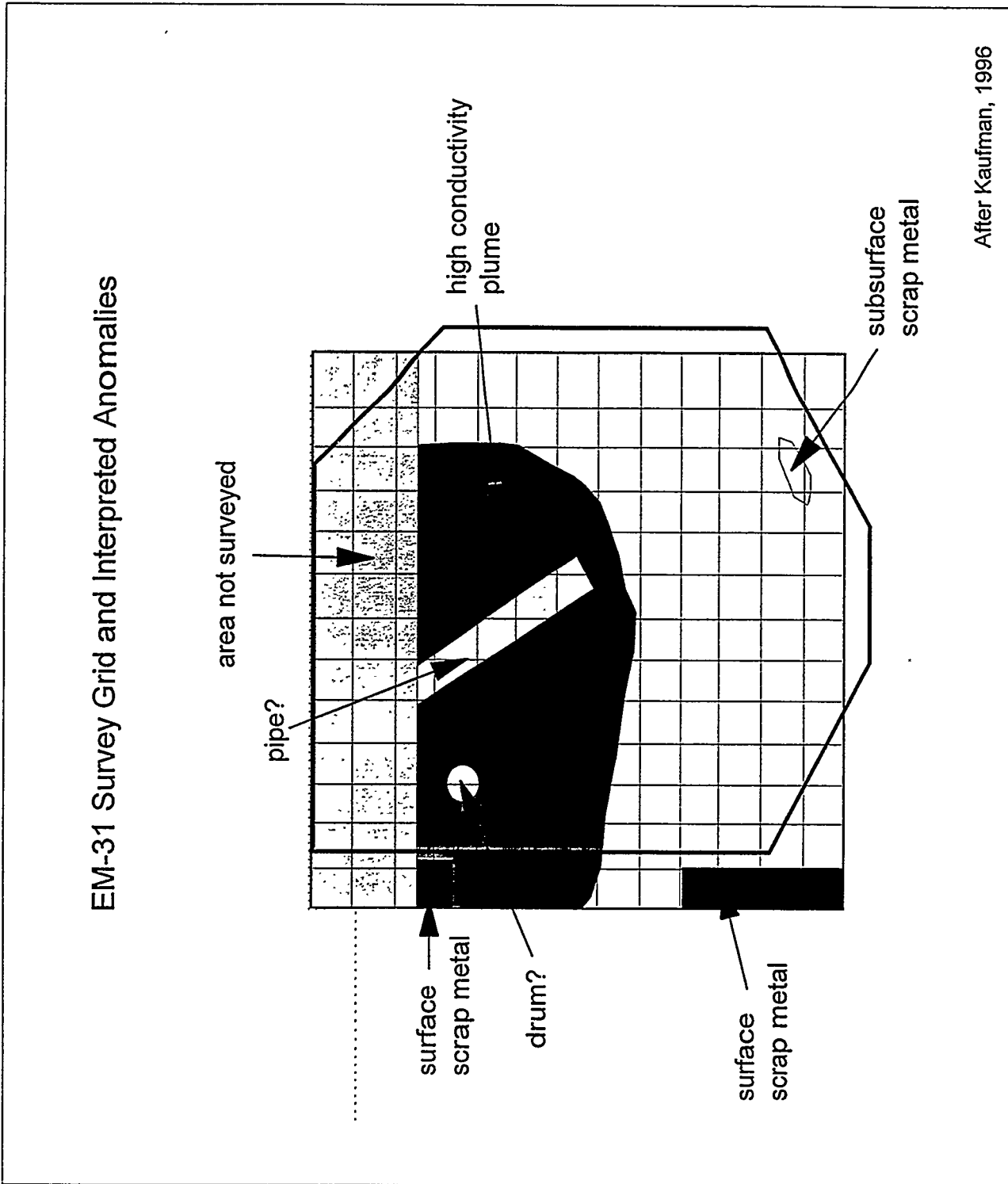


Figure 12. Results of an electromagnetic survey showing high conductivity regions and probable interpretations. The outline of the asphalt cap is shown.

2. HYDROLOGIC INVESTIGATION METHODS

2.1. Site instrumentation

Due to budgetary constraints, the pre-barrier hydrologic investigations required the use of preexisting site instrumentation (Figure 13). The only access to the interior of the impoundment beneath the asphalt cap is through a single standpipe that penetrates the cap at the center of the impoundment (I2, Fig. 13). Shallow groundwater monitoring at the water table interval was conducted by means of a network of standpipes (labeled S1 through S10 in Figure 13) that penetrate the asphalt cap but are immediately outside of the impoundment itself. All standpipes are three-inch diameter steel pipes with one-inch diameter holes drilled along the subsurface length at one-foot spacings. This construction affords sufficient connection with the surrounding groundwater to allow rapid response during transient events, as evidenced by the continuous water level data, but flow through the well is likely to be more limited than that of a screened well. Shallow groundwater below the water table interval is accessible through a network of screened monitoring wells, also shown on Figure 13. Well and standpipe construction information is summarized in Table 1.

2.2. Tracer testing: initial and second injection

On June 6, 1996, a helium gas tracer test was initiated to provide confirmation that contaminants were leaking out of the impoundment and to identify contaminant transport pathways and patterns. The central standpipe (I2) was instrumented with a passive gas injection system [Sanford et al., 1996] consisting of a central riser constructed of 1-in. PVC pipe and screen around which 400 ft of 1/8-in Teflon tubing was wrapped. Helium was continuously injected from a gas cylinder through the tubing and back to the surface, where it discharged to the atmosphere. As gas diffuses through the gas-permeable tubing, it saturates the surrounding water in the wellbore. Similar injection systems have been used successfully for gas tracer tests at Bear Creek Valley, WAG 5, and WAG 4 sites [Moline and Schreiber, 1996; Sanford et al., 1996; Knowles et al., 1995; Jardine et al., 1995; Huff and Sanford, 1995]. Gas injection began on June 6, one day after the EPA initiated dye tracer injections. Samples were obtained from multiple locations using passive diffusive samplers [Sanford et al., 1996]. This method allows the gas tracer to be extracted and brought to the laboratory for analysis without disturbing the flow system. Analysis was done by direct injection into a gas chromatograph (GC) in ESD laboratories. All of the wells and standpipes shown in Figure 13 were used for monitoring. Initial background samples were obtained prior to injection. Following injection, samples were obtained twice a week for the first six weeks of the test, and less frequently thereafter through the end of FY96. Helium injection continued through the end of FY96.

A second helium injection was initiated on March 12, 1997 and continued through June 25, 1997. The injection was delayed initially due to the need to move the location of the GC equipment. Subsequently, problems in the GC injection line developed and a new sampling method was required to allow syringe injection into the GC. Several methods were tested before developing a sampler and sampling method that adequately prevented leakage. The modified sampler is similar to the original passive diffusive device, except that the sealed end of the

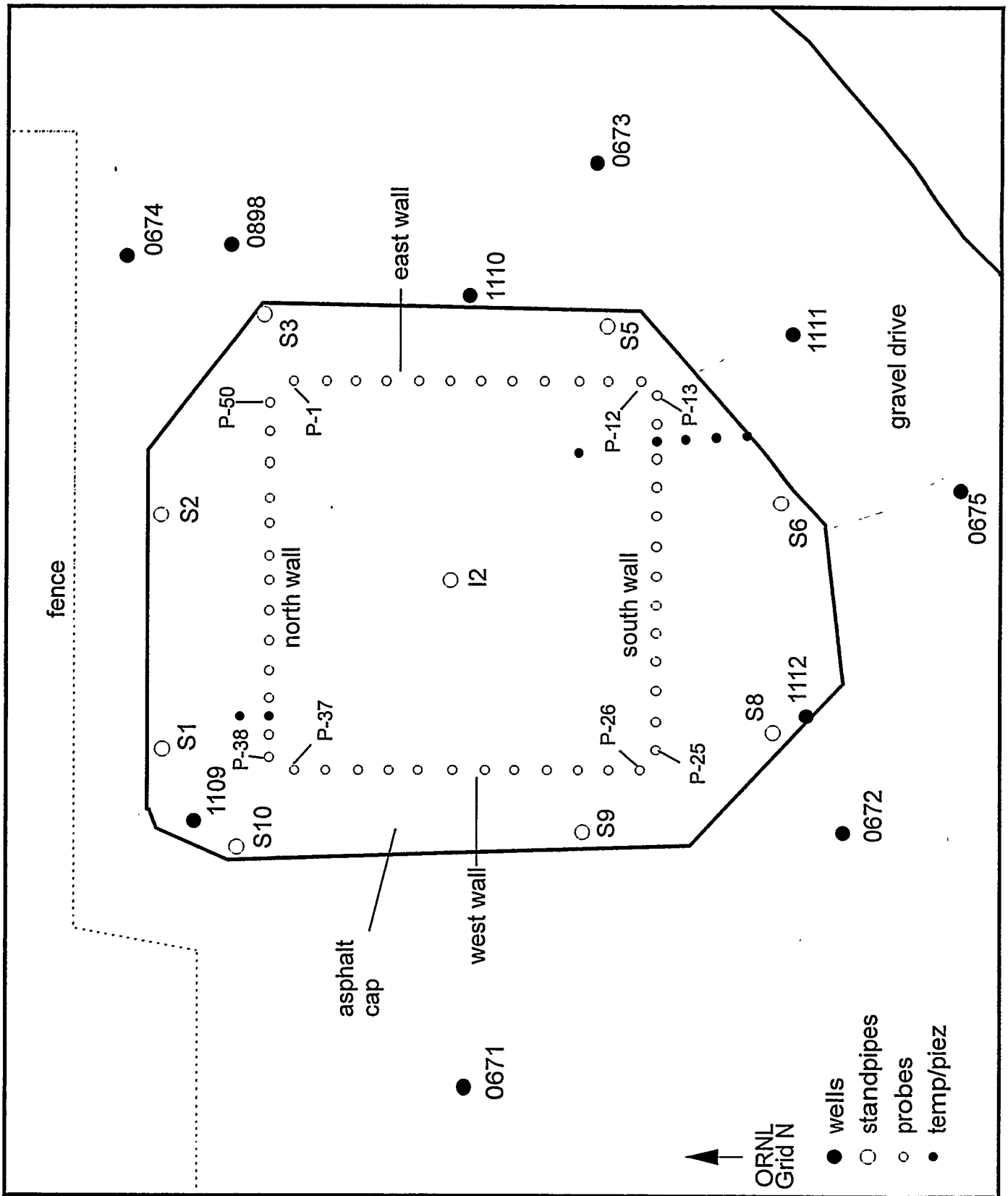


Figure 13. HRE-Pond site configuration.

well	Eastings	Northings	Grd elev	Mp elev	Depth
I2	31475.08	18585.19	818.53	822.39	17.77
S1	31433.45	18641.80	822.70	826.73	15.10
S2	31487.11	18640.32	817.86	821.85	13.65
S3	31532.40	18622.46	813.56	817.44	15.10
S5	31531.11	18556.26	813.03	817.00	16.65
S6	31496.69	18522.25	811.98	815.95	17.85
S8	31438.51	18519.74	813.22	817.19	17.90
S9	31417.97	18561.36	818.83	822.81	10.82
S10	31416.20	18631.13	823.09	827.30	10.75
0670	31450.94	18697.47	826.02	827.96	40.01
0671	31365.71	18581.74	820.94	822.94	34.24
0672	31420.23	18508.96	812.47	814.97	23.62
0673	31561.94	18556.40	806.99	808.46	27.83
0674	31542.63	18647.27	809.30	812.15	17.45
0675	31493.50	18486.97	808.22	809.58	22.80
0898	31544.78	18627.49	810.16	811.78	12.50
1109	31422.87	18634.87	823.20	827.00	29.70
1110	31533.62	18581.39	813.40	815.70	24.90
1111	31525.86	18518.64	808.10	810.80	24.70
1112	31444.65	18515.45	813.10	816.10	24.70

Table 1. Well construction information.

copper tube was replaced with a Mininert syringe valve through which the gas samples were extracted in the field using a gas-tight syringe. All connections were sealed with epoxy.

2.3. Piezometric monitoring: manual and automatic

Manual water level measurements were obtained at 20 locations from June through September, 1996 in conjunction with gas tracer sampling events (Table 2). Due to the intermittent nature of the measurements, a true storm response could not be determined. However, these data did indicate that the water table in and around the impoundment was very responsive to storms and that it probably intersected the gravel layer beneath the asphalt cap during storms, providing a pathway for rapid migration of contaminants out of the impoundment to the groundwater and surface water systems. In December of 1996, many of the wells and standpipes were instrumented with pressure transducers and temperature probes for continuous recording to more clearly define the subsurface hydrology. Seven wells were instrumented with Troll monitoring systems that record water level and temperature at 15-minute intervals. Two additional wells were instrumented with Druck transducers and Telog data loggers that recorded water levels only at 3-hour averages. The Telogs were later reprogrammed to obtain hourly averages to provide better time resolution.

2.4. Drilling logs/geologic reconstruction

On May 8, 1997, drilling began for first phase of the cryogenic barrier installation. Fifty-six boreholes were drilled to a total depth of 32 feet for the installation of 50 thermal probes and six strings of temperature probes, and an additional two holes were drilled to a total depth of nine feet for the installation of piezometers. In most cases, the holes were augered down to refusal and air-rotary drilled (ARD) to the total depth. During augering, the radiation levels were continually monitored by the HP, and soils were classified as Category I (< 1 mRad/hr), Category II (> 1 mRad/hr), or Category III (> 5 mRad/hr). Category II soils were disposed of in the pit just north of the impoundment, and Category III soils were contained in a B-52 box. ARD was done using a closed system where cuttings and drill water were piped directly into a container, so no monitoring or logging were possible through these intervals. Geologic logging was completed for the majority of the boreholes, which included a general soil description and the radiation category. The borehole logs were used to construct geologic cross sections along each wall of the impoundment to aid in interpreting the subsurface hydrology and the location of primary contaminant transport pathways.

3. HRE-POND HYDROLOGY

3.1. Water table configuration

Figure 14 shows a dry season water table map and measured hydraulic heads for July 8, 1996. In an isotropic porous medium, groundwater flow would be perpendicular to the hydraulic head contours. This may be a reasonable gross representation for flow through the fill materials within and overlying the impoundment, where any structure that might have been present in the original material would have been destroyed. However, flow through the undisturbed shale bedrock and overlying saprolite surrounding the impoundment will be heavily influenced by a fracture

Table 2. HRE-Pond Water Levels (ft above msl)

date	I-2	S-1	S-2	S-3	S-5	S-6	S-8	S-9	S-10
5/1/96	815.14	818.91	813.40	812.01	811.35	803.57	807.04	812.49	819.72
6/6/96	814.30	817.25	813.08	811.30	809.52	803.39	806.14	812.19	818.82
6/10/96		819.22	813.31	812.01	811.77	803.52	807.31	812.32	820.37
6/13/96		819.19	813.32	811.97	811.60	803.54	807.31	812.42	820.15
6/17/96		818.30	813.08	811.56	809.98	803.46	806.53	812.28	818.92
6/20/96		817.26	813.06	811.36	809.59	803.40	806.24	812.23	818.83
6/25/96		817.16	813.02	811.73	810.81	803.27	807.50	812.09	819.04
7/1/96		817.12	812.97	811.28	809.57	803.20	806.21		818.82
7/8/96		817.05	812.96	810.85	808.90	803.07	805.67		818.67
7/11/96		817.00	812.93	810.75	808.67	803.01	806.20		818.64
7/15/96		817.04	812.92	812.16	809.09	803.28	807.70	812.83	819.17
7/18/96		817.50	813.00	811.71	810.06	803.41	806.65	812.23	819.02
7/22/96		819.06	813.22	812.16	812.01	803.53	807.60	812.77	820.32
7/25/96		818.26	813.15	811.65	809.62	803.49	806.54	812.25	819.02
7/29/96		819.20	813.39	812.11	811.61	803.54	807.40	812.50	820.23
8/1/96	816.39	819.40	813.59	812.06	811.96	803.95	807.69	812.79	821.08
8/8/96	814.94	817.29	813.06	811.38	809.32	803.47	806.18	812.24	818.88
8/27/96	815.21		813.10	811.89	810.00	803.48	806.84		

date	670	671	672	673	674	675	898	1109	1110	1111	1112
12/20/95		815.82			810.24	802.73					
12/22/95	814.61										
1/23/96		814.84			809.87	802.56					
1/25/96	814.83										
2/27/96		814.40			809.64	802.52					
2/29/96	814.30										
3/20/96		815.33			810.00	802.68					
3/21/96	814.56										
4/19/96	814.18	814.51			809.73	802.51					
5/1/96		814.94		808.44	809.64	802.08	808.98	813.72	808.11	803.56	804.83
5/21/96		814.51			809.65	802.46					
5/22/96	813.98										
6/6/96		814.26	805.86	807.79	809.51	801.85	808.56	812.56	807.36	803.14	804.64
6/10/96		816.25	806.23		810.20	802.77	809.59		808.94	804.07	805.15
6/13/96		815.87	806.79		809.97	802.70	809.43		808.83	803.88	805.14
6/17/96		814.96	806.00		809.78	802.50	808.91		808.07	803.36	804.88
6/19/96	814.13	814.65			809.67	802.44					
6/20/96		814.51	805.86	807.79	809.63	802.40	808.70			803.33	804.79
6/25/96		814.23	805.79	807.68	809.61	802.40	808.69		807.63	803.23	804.56
7/1/96		813.93	805.49	807.67	809.30	802.28	808.27			803.06	804.50
7/8/96		813.69	805.29	807.17	809.07	802.11	808.05		807.03	803.11	804.37
7/11/96		813.61	805.39	807.12	808.97	802.13			807.03	802.87	804.33
7/15/96		814.27	805.64	807.71	809.69	802.31	808.63		807.27	803.13	804.62
7/17/96	814.11	814.47			809.73	802.37					
7/18/96		814.44	805.75	807.63	809.71	802.36	808.71		807.67	803.25	804.78
7/22/96		814.85	805.94		810.04	802.65	809.25		808.28	803.52	804.97
7/25/96		814.75	805.74	807.98	809.77	802.45	808.90		807.98	803.29	804.86
7/29/96		815.55	806.09		810.11	802.70	809.37		808.69	803.81	805.11
8/1/96		816.89	806.32		810.42	803.13	809.78	816.19		804.26	805.33
8/8/96				808.21	809.68	802.40	808.74	812.99	807.55	803.30	804.81
8/19/96		814.58			809.64	802.42					
8/22/96	813.72										
8/27/96				808.21	809.74		808.86	813.09	807.66	803.31	

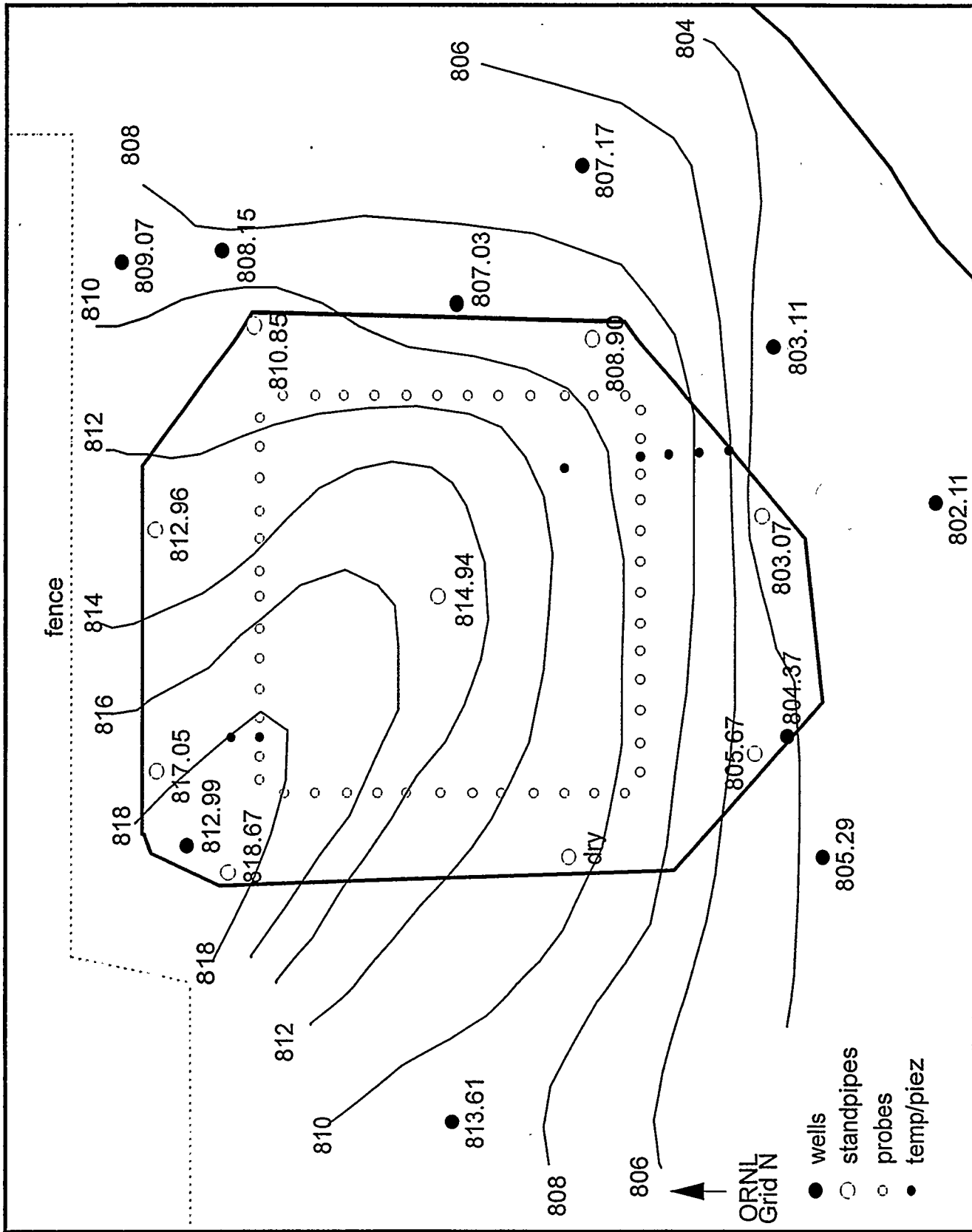


Figure 14. Dry season water table elevation on 7/8/96 (ft above msl).

network that induces significant anisotropy and strike-preferential flow in similar materials on the Oak Ridge Reservation.

Composite hydrographs for the standpipes and wells derived from manual water level measurements are shown in Figures 15 and 16, respectively. These data indicate downward gradients along all margins of the cap, and upward gradients east of the impoundment close to the tributary. For example, well 0673 is flowing during much of the winter wet season. These downward gradients surrounding the impoundment indicate that any contaminants that may leak from the impoundment would be likely to be carried downward through the shallow groundwater system to some extent before being discharged to nearby tributaries. On average, water levels were only slightly higher in the winter months of 1996-97, and the pattern of hydraulic heads does not change significantly. However, direct comparison of continuous and manual water level measurements is difficult at best, and the continuous water level measurements for the summer of 1997 represent conditions that were disturbed by drilling and installation of the cryogenic barrier probes.

3.2. Storm response

Although seasonal variations in the water table are small, storm-driven variations are quite large in many wells. Figures 17 through 26 show hydrographs for each of the wells equipped with continuous water level monitoring devices. All but two logging devices also recorded temperature variations. Two of the monitoring devices were moved from their original locations to obtain data at other locations, resulting in short records for those locations. Comparison of these hydrographs with those obtained from manual measurements demonstrates that much of the storm response is not captured without continuous monitoring. In many cases, the peak storm response occurs over a period of a few hours and may be as much as 3.5 ft (e.g., Figs. 20 and 22).

Several conclusions can be drawn from the well hydrographs. First, the rise in water table in some locations is large enough to intersect the gravel layer, as was previously hypothesized (Moline, 1996), and is therefore likely to be driving episodic contaminant release from the impoundment through this high-permeability layer. This release could occur either through the transport of fine sediment to which radionuclides are sorbed, or through the flushing of water that remains in the sediments between storm events and provides a means for leaching radionuclides from the soils. An example of the rapid storm response can be seen in the hydrograph for the center standpipe I2 (Figure 23). The elevation of the asphalt cap is 818.5 ft at this location, and the storm-driven water levels often exceed 817 ft which is a conservative estimate for the bottom of the gravel layer at this location based on an assumption of a one-foot thickness. A more likely estimate is 816 ft, where the slope of the recession curve changes sharply as discussed in the following section. Second, water temperature fluctuations associated with storm events demonstrate that significant groundwater flux is moving through the system during these events. The response is seen more clearly during winter months due to the more pronounced temperature differences between the ambient groundwater and the infiltrating precipitation. Third, the elevation of the water table exceeds the elevation of the original impoundment. Therefore, the fill above the original impoundment is saturated during and between storm events, providing a

Hydraulic Heads: Stand pipes

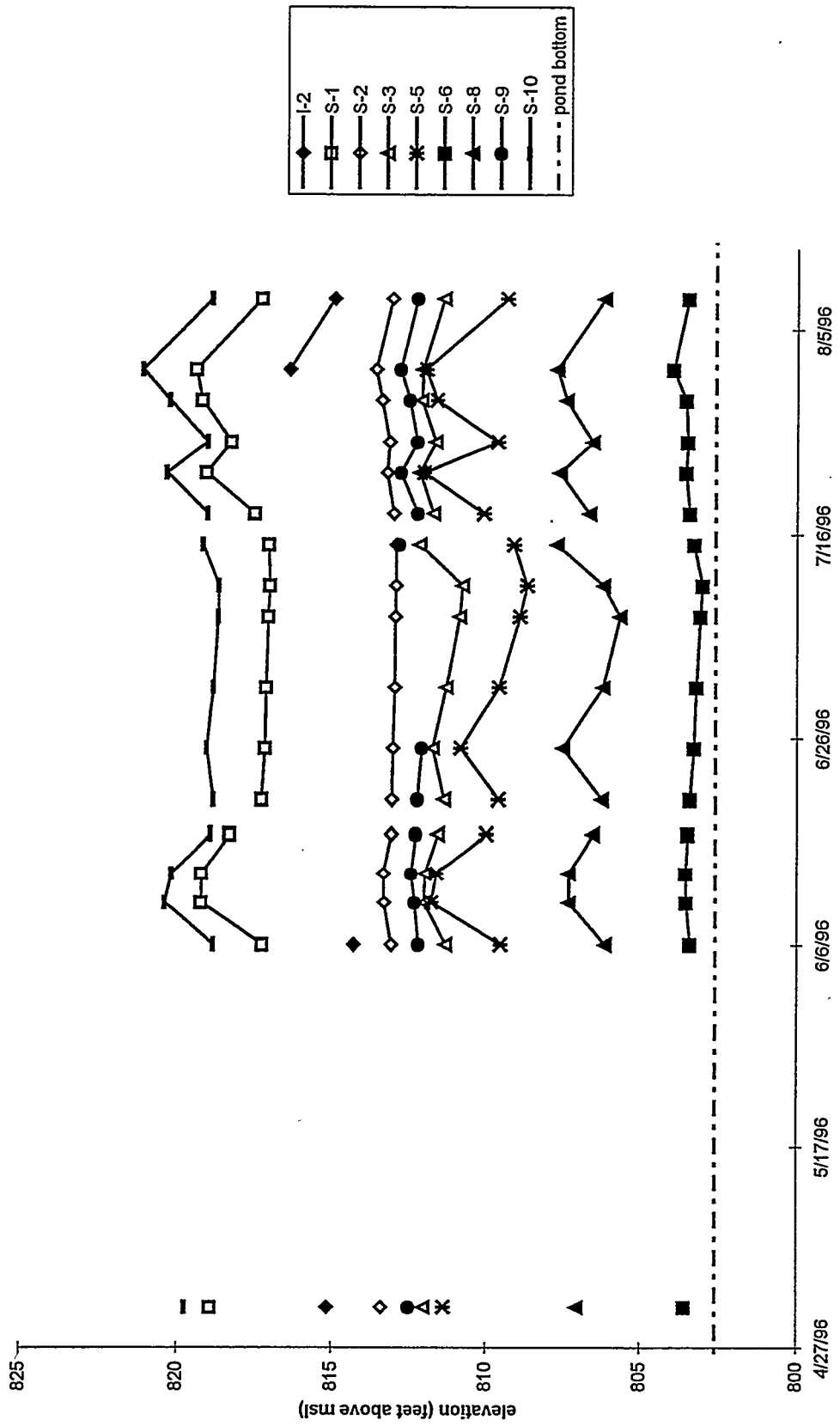


Figure 15. Water levels in HRE-Pond stand pipes. Note that all levels exceed the bottom of the impoundment.

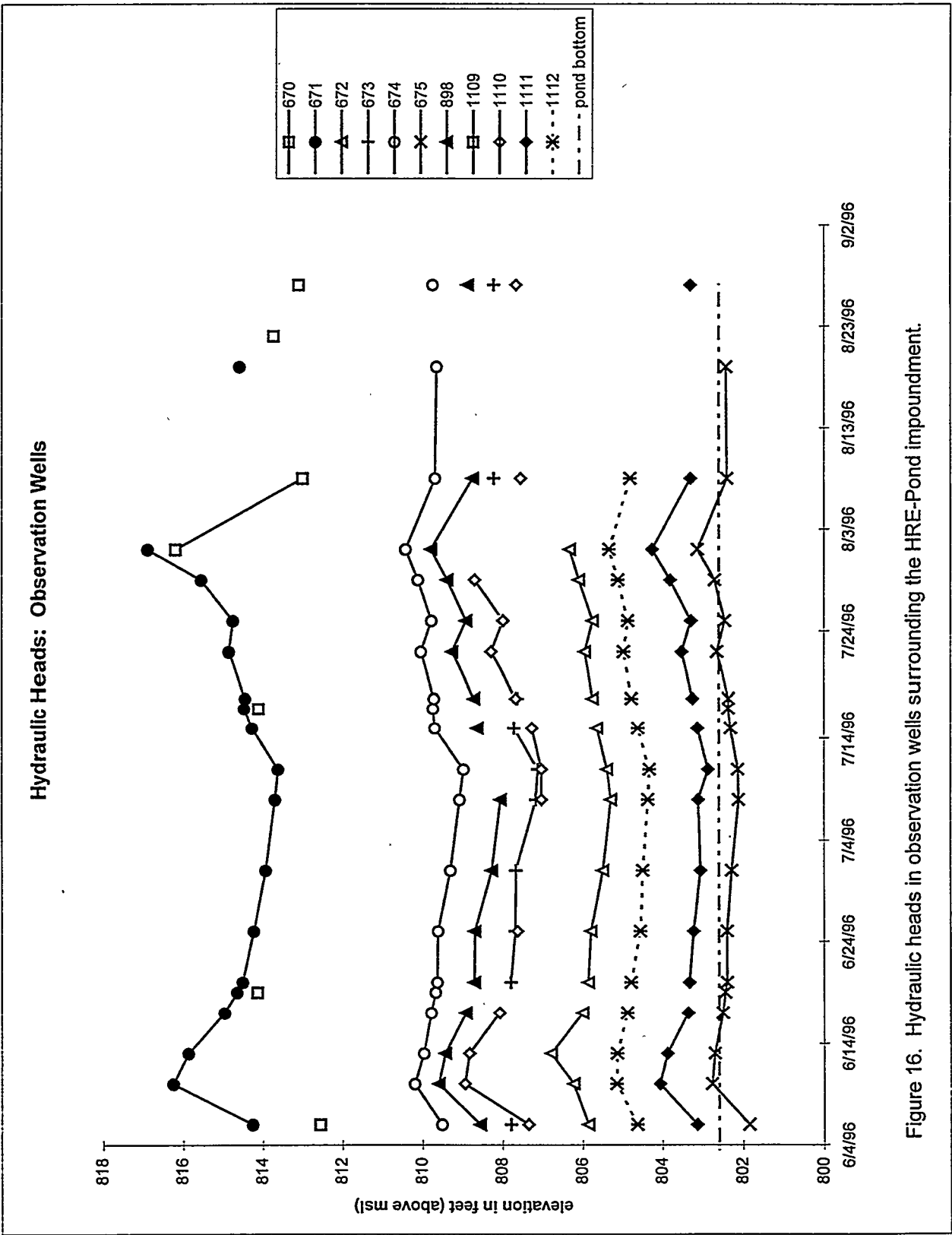


Figure 16. Hydraulic heads in observation wells surrounding the HRE-Pond impoundment.

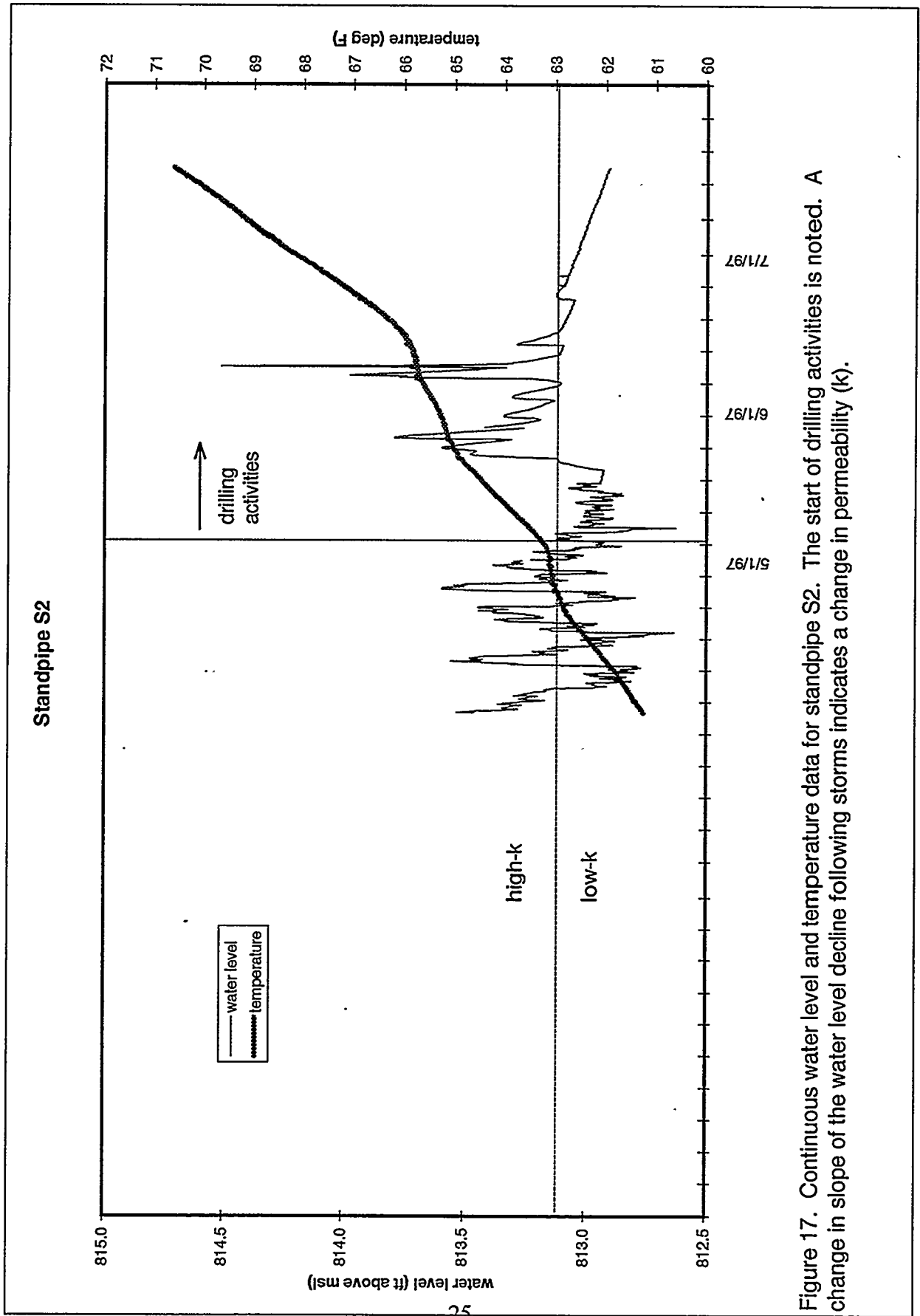


Figure 17. Continuous water level and temperature data for standpipe S2. The start of drilling activities is noted. A change in slope of the water level decline following storms indicates a change in permeability (k).

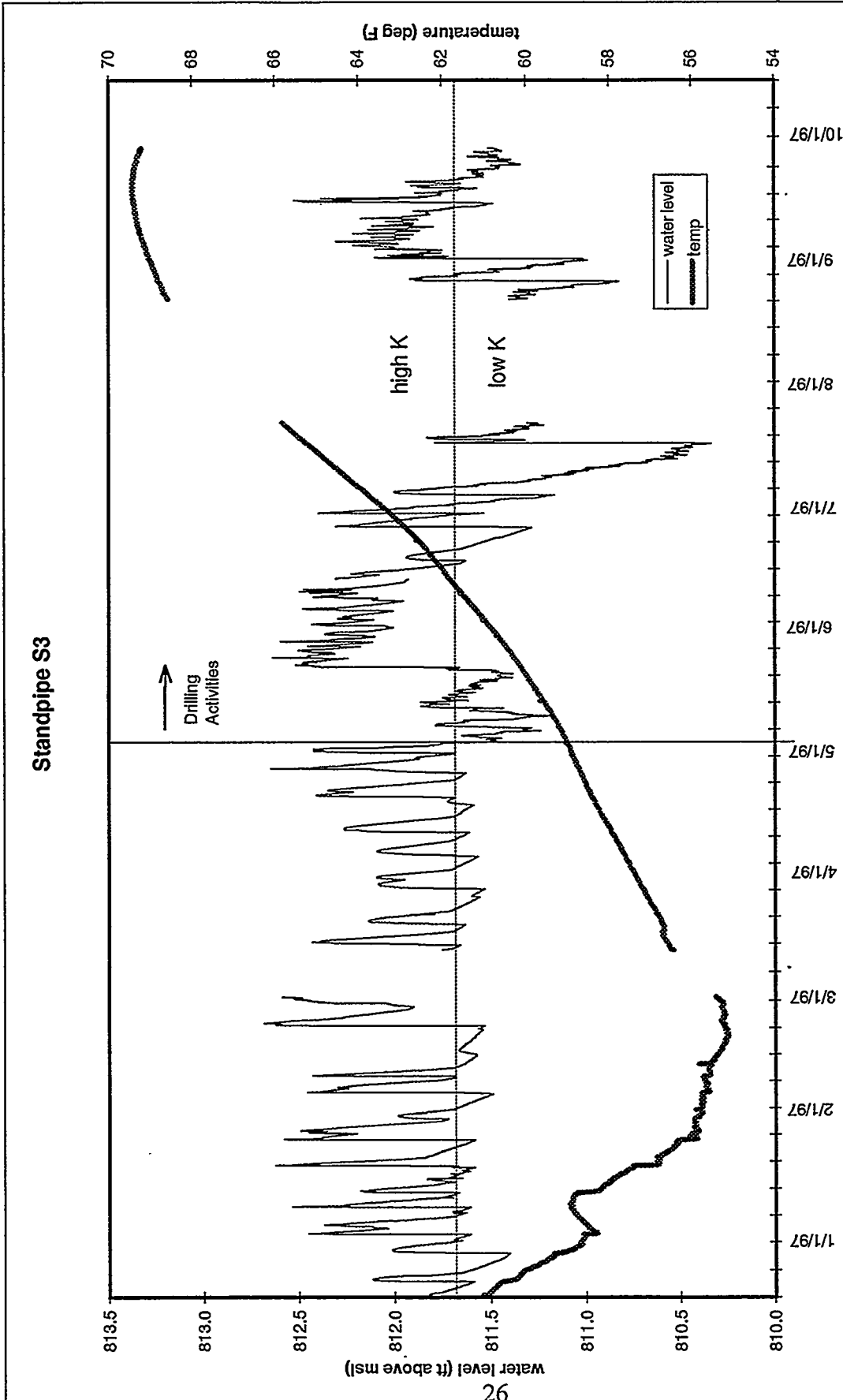


Figure 18. Continuous water level and temperature data for standpipe S3. The start of drilling activities is noted. A change in slope of the water level decline following storms indicates a change in permeability (k).

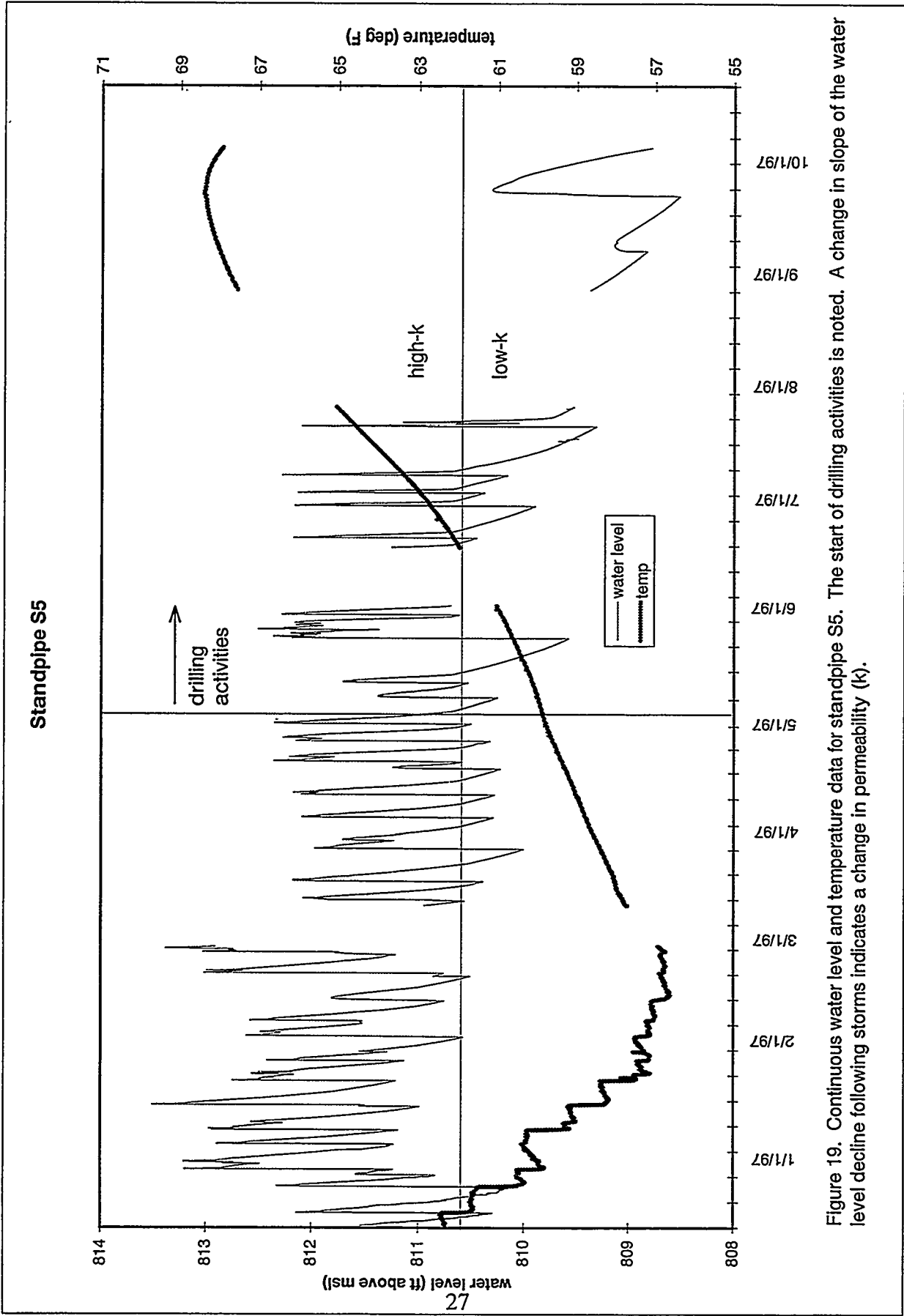


Figure 19. Continuous water level and temperature data for standpipe S5. The start of drilling activities is noted. A change in slope of the water level decline following storms indicates a change in permeability (k).

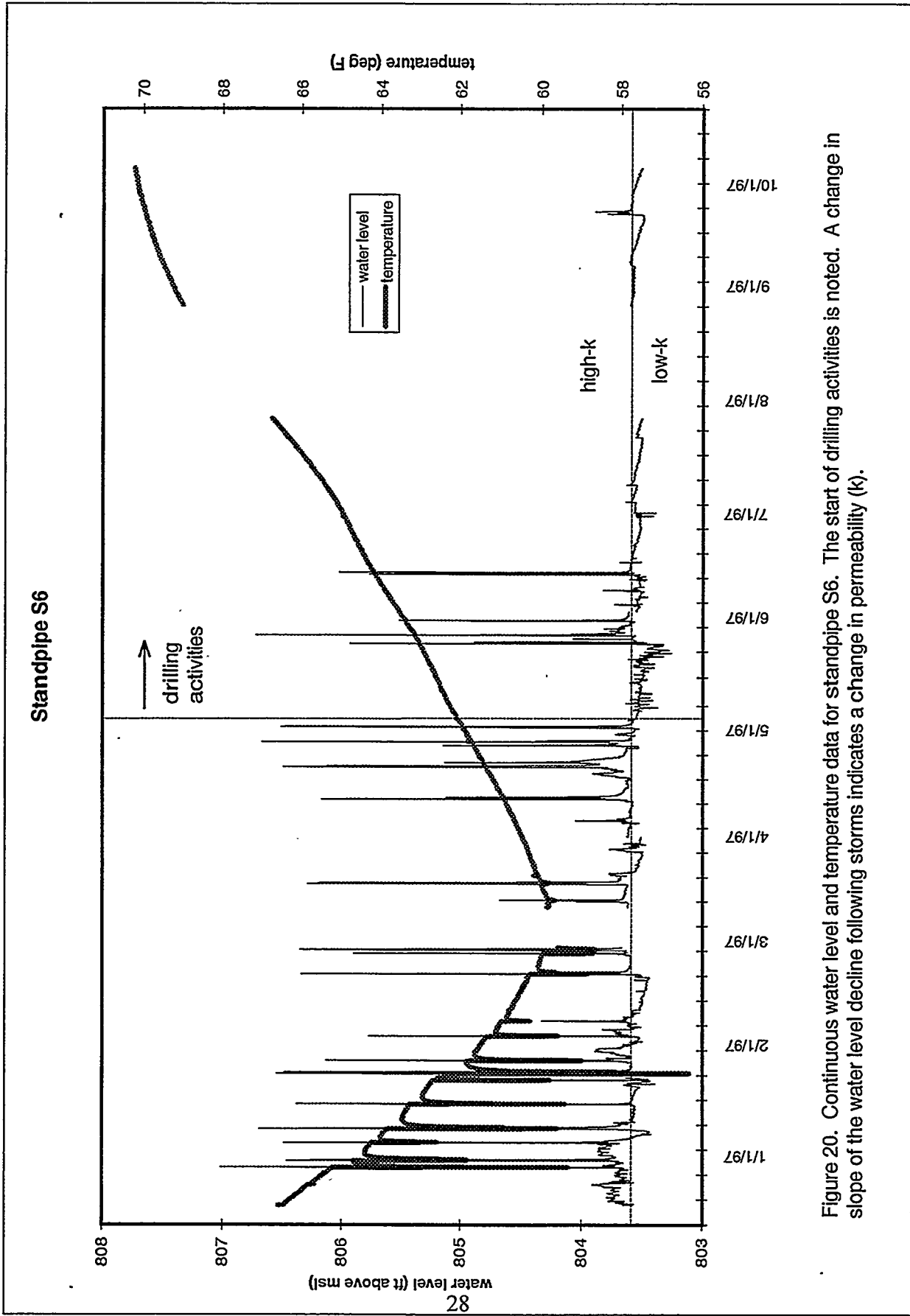


Figure 20. Continuous water level and temperature data for standpipe S6. The start of drilling activities is noted. A change in slope of the water level decline following storms indicates a change in permeability (k).

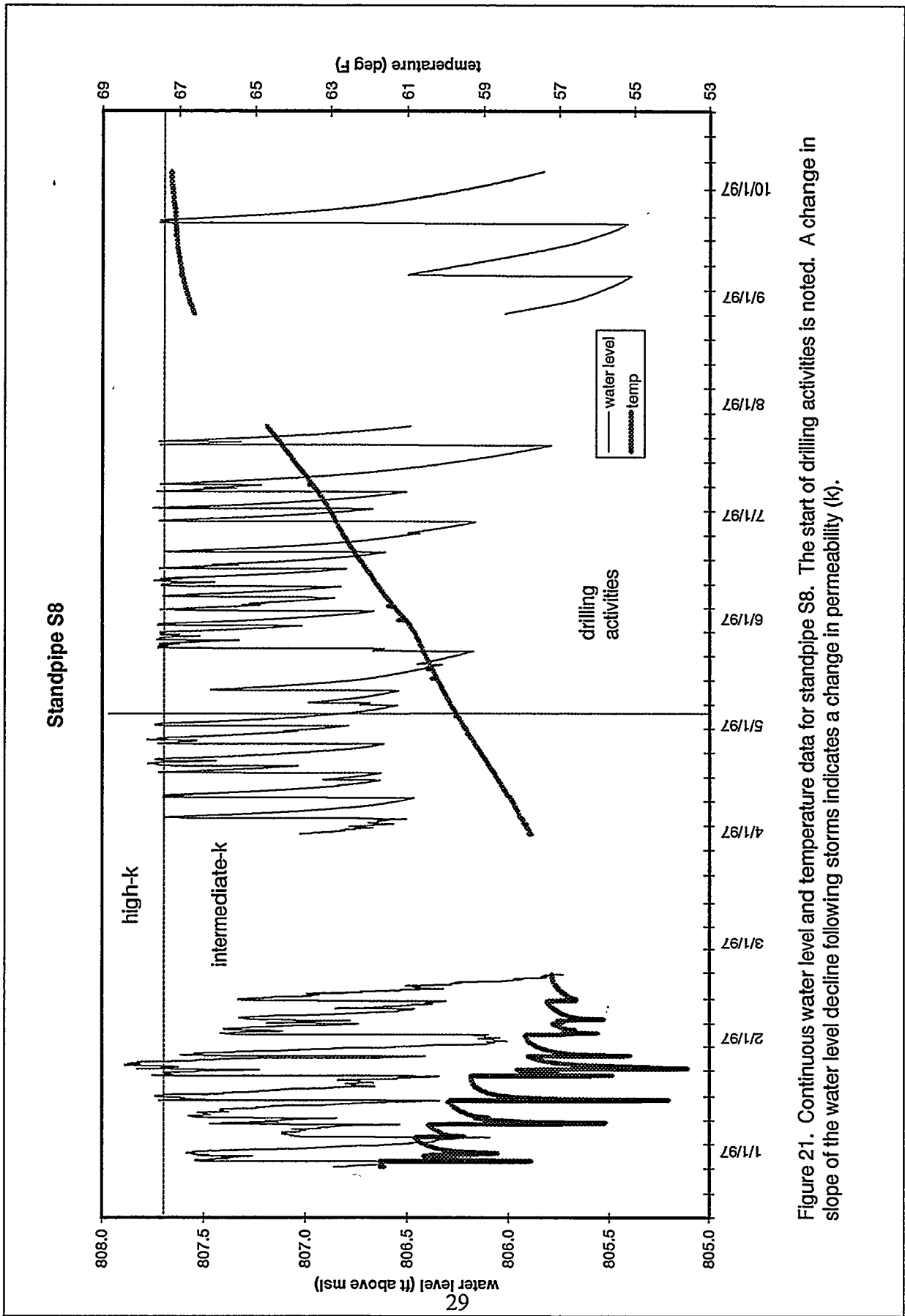


Figure 21. Continuous water level and temperature data for standpipe S8. The start of drilling activities is noted. A change in slope of the water level decline following storms indicates a change in permeability (k).

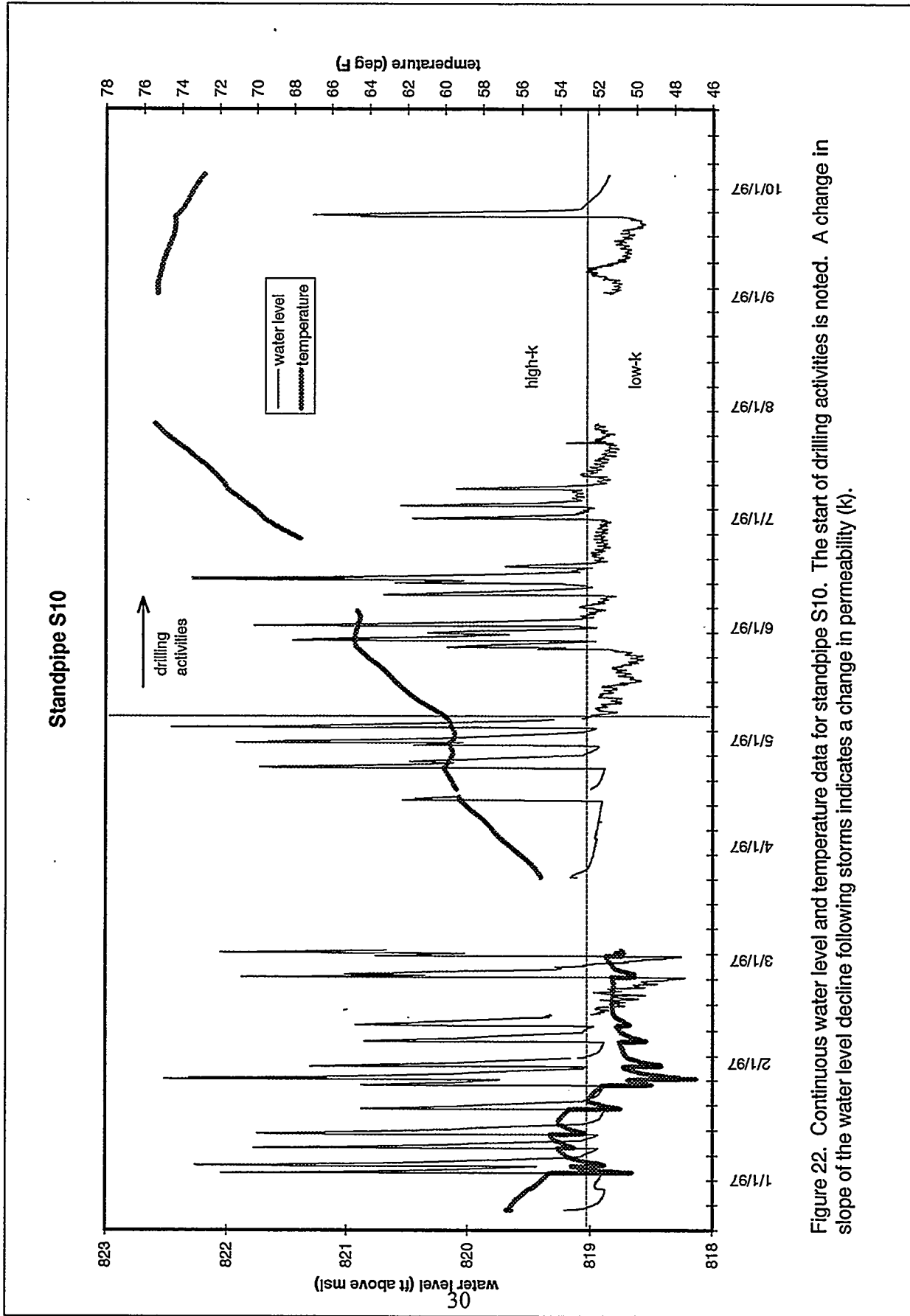


Figure 22. Continuous water level and temperature data for standpipe S10. The start of drilling activities is noted. A change in slope of the water level decline following storms indicates a change in permeability (k).

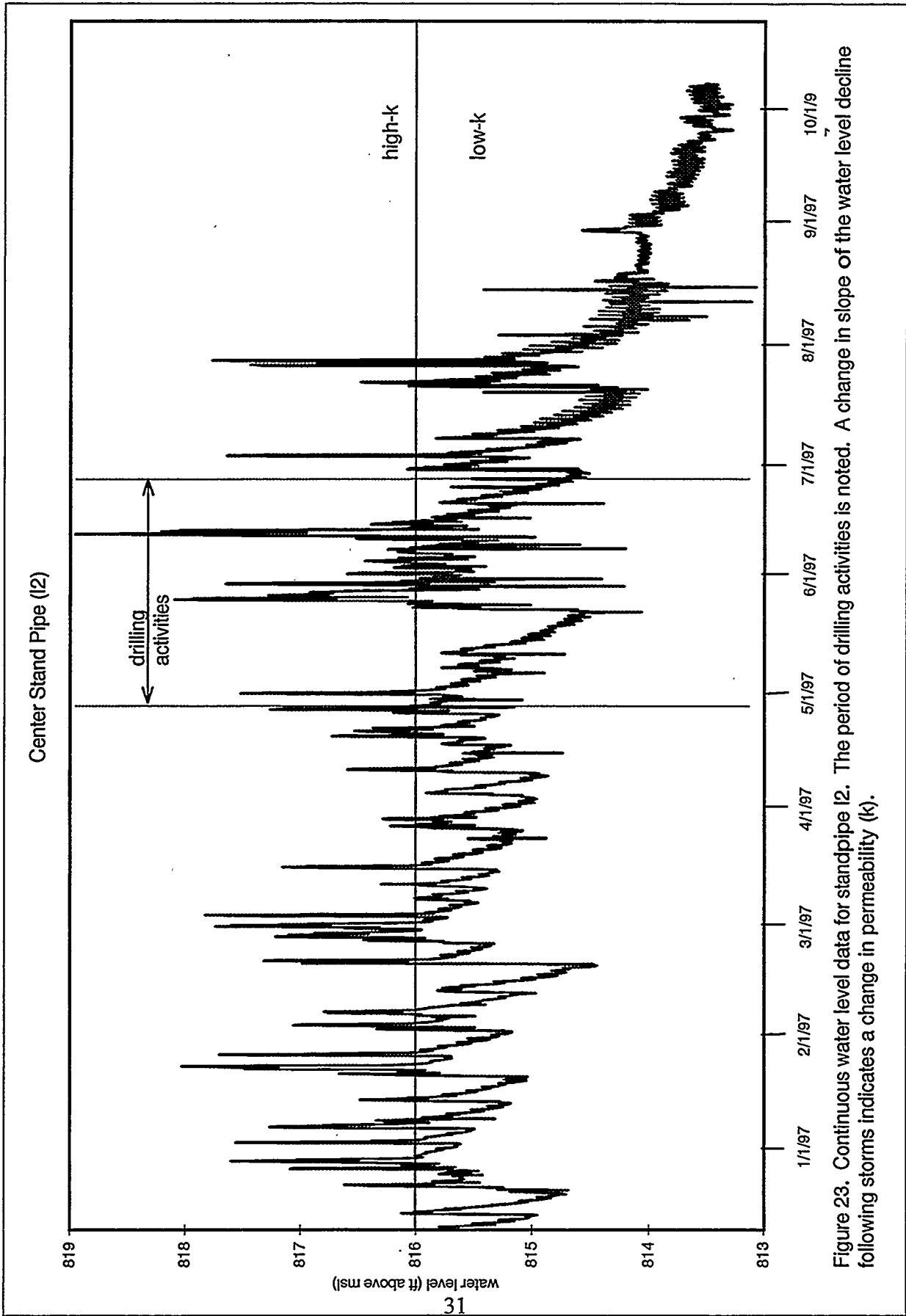


Figure 23. Continuous water level data for standpipe I2. The period of drilling activities is noted. A change in slope of the water level decline following storms indicates a change in permeability (k).

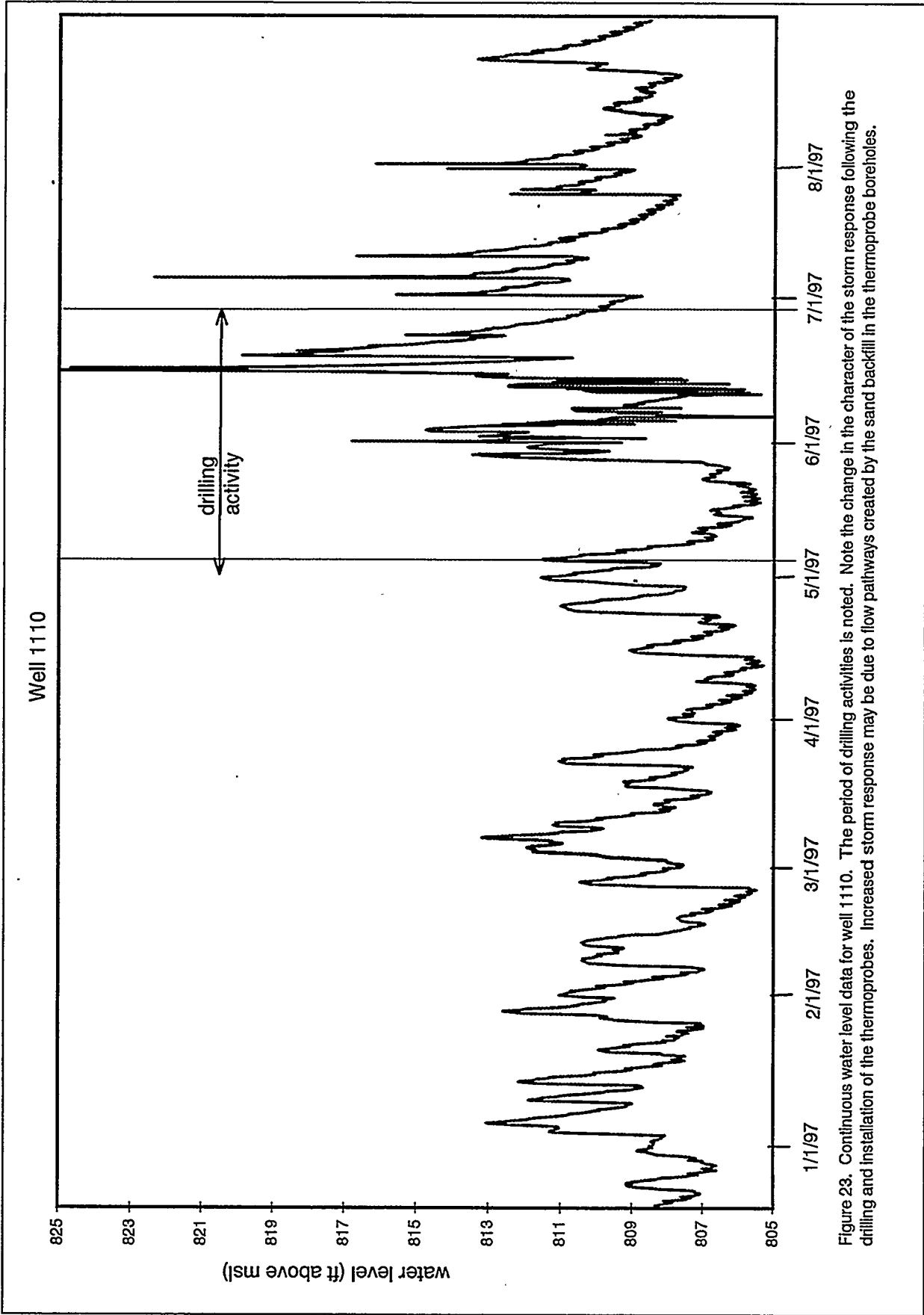


Figure 23. Continuous water level data for well 1110. The period of drilling activities is noted. Note the change in the character of the storm response following the drilling and installation of the thermoprobes. Increased storm response may be due to flow pathways created by the sand backfill in the thermoprobe boreholes.

Well 0673

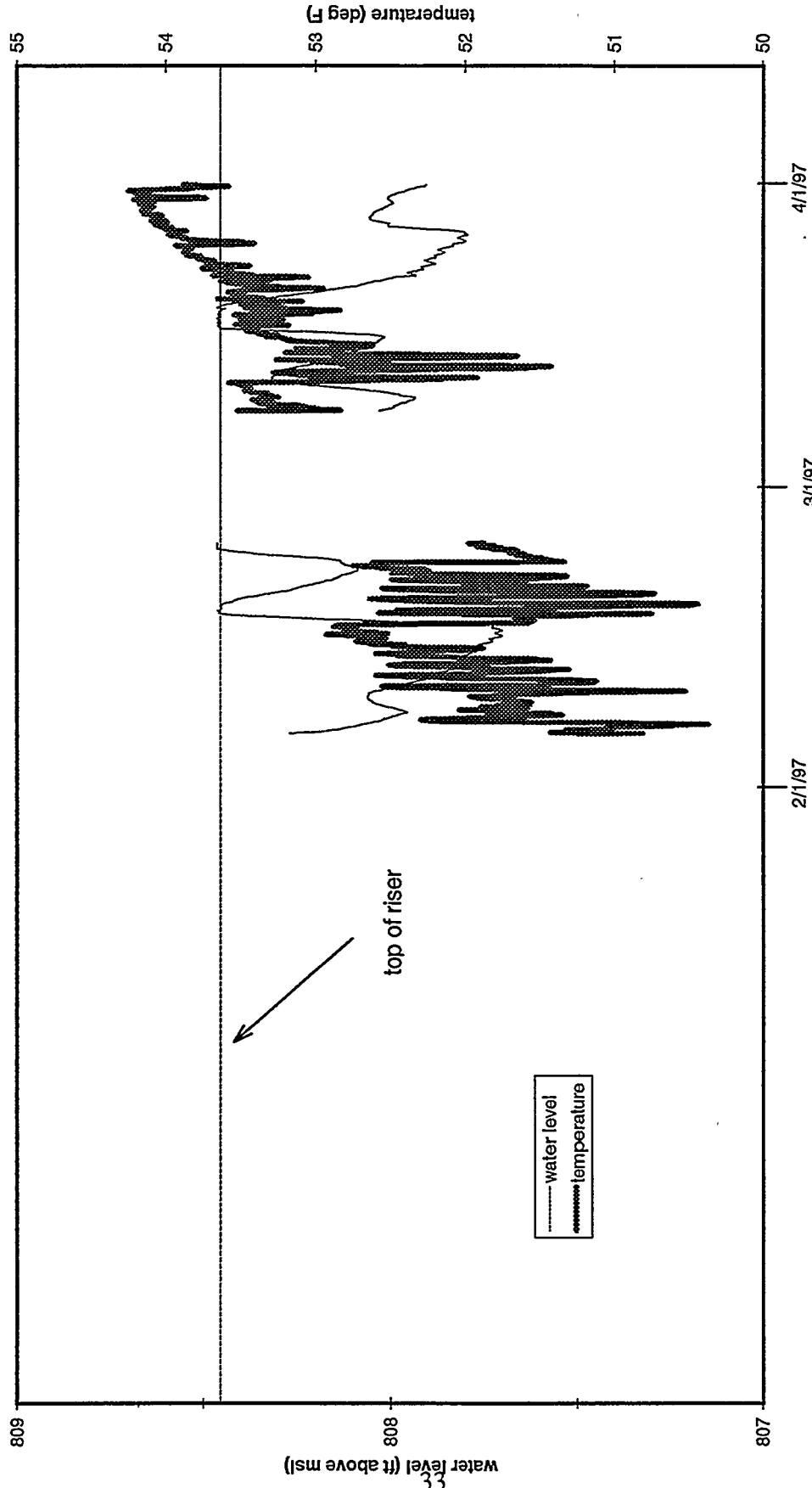


Figure 25. Continuous water level and temperature data for well 0673. The line indicates the elevation of the top of the riser. Above that level, the well was flowing.

Well 0898

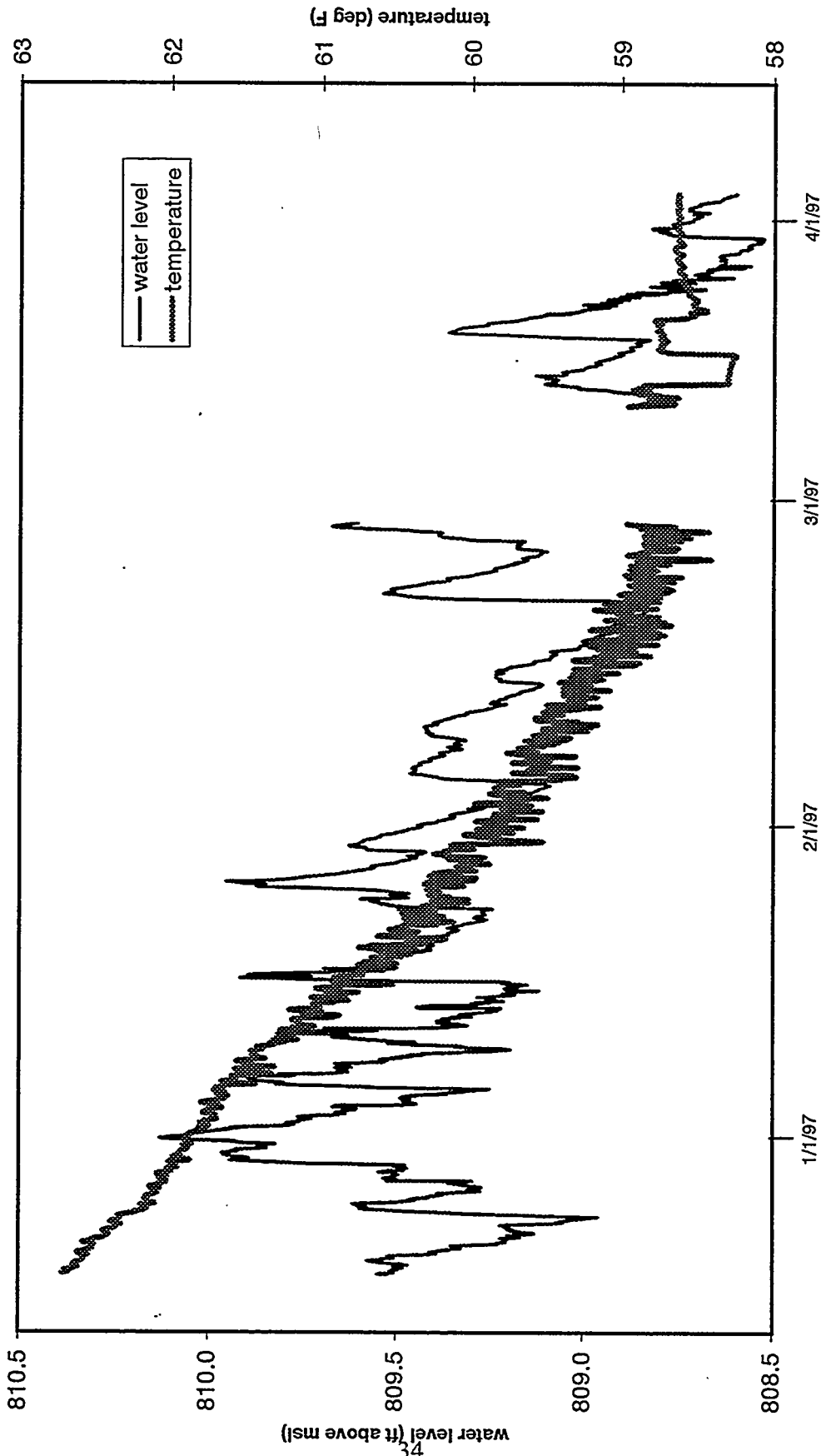


Figure 26. Continuous water level and temperature data for standpipe S3. Due to excessive noise, the temperature data have been smoothed using a 12-hour moving window average.

transport pathway for contaminants from the impoundment if the fill is transmissive enough to allow significant groundwater flux. The rapid decline in water levels in and around the impoundment following storm events indicates that the materials saturated during these events are, in fact, significantly transmissive.

3.3. Hydraulic conductivity

The majority of the hydrographs exhibit definite breakpoints in the slope of the recession curves following storm events. Several of the hydrographs demonstrate the consistency of the storm recession slopes and breakpoint elevation over a series of storm events. Where noted, these breakpoints are indicated on the hydrographs by a dashed line. Breakpoints and recession slopes can provide an indication of the relative hydraulic conductivity of various regions in and around the impoundment because the rate at which the water added to the system during a storm drains is a function of the local hydraulic conductivity and storativity. For example, Shevenell et al. [1996] used breakpoints in the storm recession curves from a number of wells to determine the transmissivities of multiple pore regions in a karst terrain (e.g., conduits, fractures, and matrix pores). Similarly, the HRE-Pond well hydrographs also reflect drainage from multiple pore regions, although in this case the pore regions are more likely to be associated with changes in subsurface materials rather than changes in pore types within the same material, as is the case with the deeper karst wells. The elevation at which a breakpoint occurs indicates the elevation at which a permeability change occurs for water table wells where changes in water level can be attributed to actual dewatering in an unconfined system. This conclusion is supported by comparing the hydrographs with the geologic logs and the pond construction information.

Several of the standpipes demonstrate extreme hydraulic conductivity differences. S-6 (Figure 20) and S-10 (Figure 22) show a rapid rise and equally rapid recovery from storm events, bottoming out at a consistent elevation. Both of these wells are located within some of the drainage ditches that were constructed around the original impoundment. These ditches would presumably have been constructed out of low-permeability material to contain any pond overflow and prevent release into the surrounding groundwater. The storm response is very similar to the type of response seen in conduit flow, and the base levels may indicate the elevation of the original ditch at that location. Conversely, water levels in S-8 (Figure 21) are cropped at the upper end, a phenomenon that is more easily seen when looking at the hourly water level readings during a storm event.

The center standpipe shows a conductivity change at around 816 ft. The slower rate of recession below that elevation may represent the elevation at which the groundwater mounding beneath the asphalt cap intersects the original clay berm and is forced to drain through lower permeability materials.

4. CONTAMINANT TRANSPORT PATHWAYS

4.1. Helium and dye tracer distribution

Due to the inability to calibrate the new sampling and analysis system before the end of the

tracer test, the results are not quantitative. However, they do provide qualitative confirmation of helium tracer transport out of the impoundment. The interpretation of the tracer test results requires the following to be considered. First, the sampling and analysis methods can lead to false negative results if water leaks into the sampler or gas is lost during or subsequent to sampling. However, there are no mechanisms that can lead to a false positive if the chromatographic peak is properly identified. Second, the tracer test data cannot be used to determine groundwater velocities. It is impossible to definitively state that the helium detected during the second injection was entirely due to the second injection because of the potential for retention of large masses of helium in the low-permeability/high-porosity materials in and around the impoundment. (This would be true of a repeat dye injection as well.) In addition, the detection limit varied because changes in the sampling and analysis methods resulted in changes in the overall volume of gas obtained and analyzed.

Table 3 summarizes the frequency of helium detects for each of the wells sampled. Despite the equipment problems incurred during the helium tracer test, the data provide important confirmation of the transport of contaminants out of the impoundment under ambient conditions. Figure 27 shows the locations where helium was detected one or more times, which are consistent with the eosin dye tracer results under initial forced-gradient conditions [Field, 1996]. The most frequent detects occurred in the standpipes (ie., water table interval) in a radially-distributed pattern, consistent with transport through either the gravel layer or the more permeable fill above the berm of the original impoundment. The lack of detection through the dry months and the episodic nature of the dye and helium tracer transport is consistent with primary transport through high permeability materials that saturate during elevated water table conditions.

The frequent detection of helium in S-10, and less frequently in S-1, in opposition to the average hydraulic gradient is enigmatic. Well 1109 also tested positive for helium, but has a lower hydraulic head than both the injection well and the adjacent standpipe, indicating a local downward gradient. The transport of helium in the gas phase within the gravel layer and subsequent dissolution into the shallow groundwater could be an explanation, except that the eosin dye tracer was also transported to S-10. This observation remains unexplained.

It is clear from the tracer data that there are multiple pathways for contaminants to be transported out of the impoundment, with rapid episodic transport likely during the winter wet season and during storm events year-round. While these data can not confirm that the radionuclide contamination in the creek is due to sources in the impoundment, they do confirm that the potential exists and that some contribution from the impoundment is highly probable.

4.2. Soil contamination patterns

Soil contamination patterns observed during the drilling of the cryo-barrier boreholes can provide insight into the possible mechanisms for contaminant leakage out of the impoundment. Fifty-six boreholes were drilled for the installation of thermoprobes and temperature probes. Boreholes were augered down to refusal (top of bedrock) in most cases followed by air rotary drilling to

Table 3. Helium Detections Following 2nd Tracer Injection

Location	#samples	#dets	17-Mar	4-Apr	11-Apr	22-Apr	24-Apr	29-Apr	2-May	15-May	27-Jun
S1	6	4	wet	wet	0	X	X	X	X	0	evac
S2	6	2	0	0	na	X	wet	0	wet	0	X
S3	7	6	X	X	X	X	X	0	wet	methane	X
S5	7	5	X	0	X	X	X	0	wet	na	tr
S6	9	5	X	0	0	X	X	X	0	0	tr
S8	7	3	0	0	na	X	0	0	X	X	na
S9	3	1	na	0	na	na	X	0	na	na	na
S10	5	2	na	na	na	na	X	0	0	0	X
I2	9	9	X	X	X	X	X	X	X	X	X
1109	7	6	X	na	0	X	X	na	X	X	X
1110	8	2	0	0	0	X	X	0	0	0	na
1111	7	6	X	X	X	X	X	na	0	X	na
1112	4	1	na	na	0	X	0	na	0	na	na
672	1	0	na	na	na	na	0	na	na	na	na
673	1	0	na	na	na	na	na	na	0	na	na
674	7	3	X	X	0	X	0	na	0	0	na
675	6	2	0	0	na	X	X	na	0	0	na
CP	4	1	X	0	na	na	na	0	0	na	na

tr = trace (peak detectable but concentration too low to count)
methane = methane peak overriding possible He peak
wet = water vapor may have suppressed the He peak
na = not sampled
evac = sample lost
#samples = number of valid samples
#dets = number of positive He detects; conc. could not be accurately quantified.
X = positive He detection
0 = non-detects

Table 3. Frequency of helium detections at the HRE-Pond monitoring locations following the 2nd tracer injection. Data are qualitative only due to changes in the design of the gas sampling device to rectify leakage problems. Locations are shown on Figure 27.

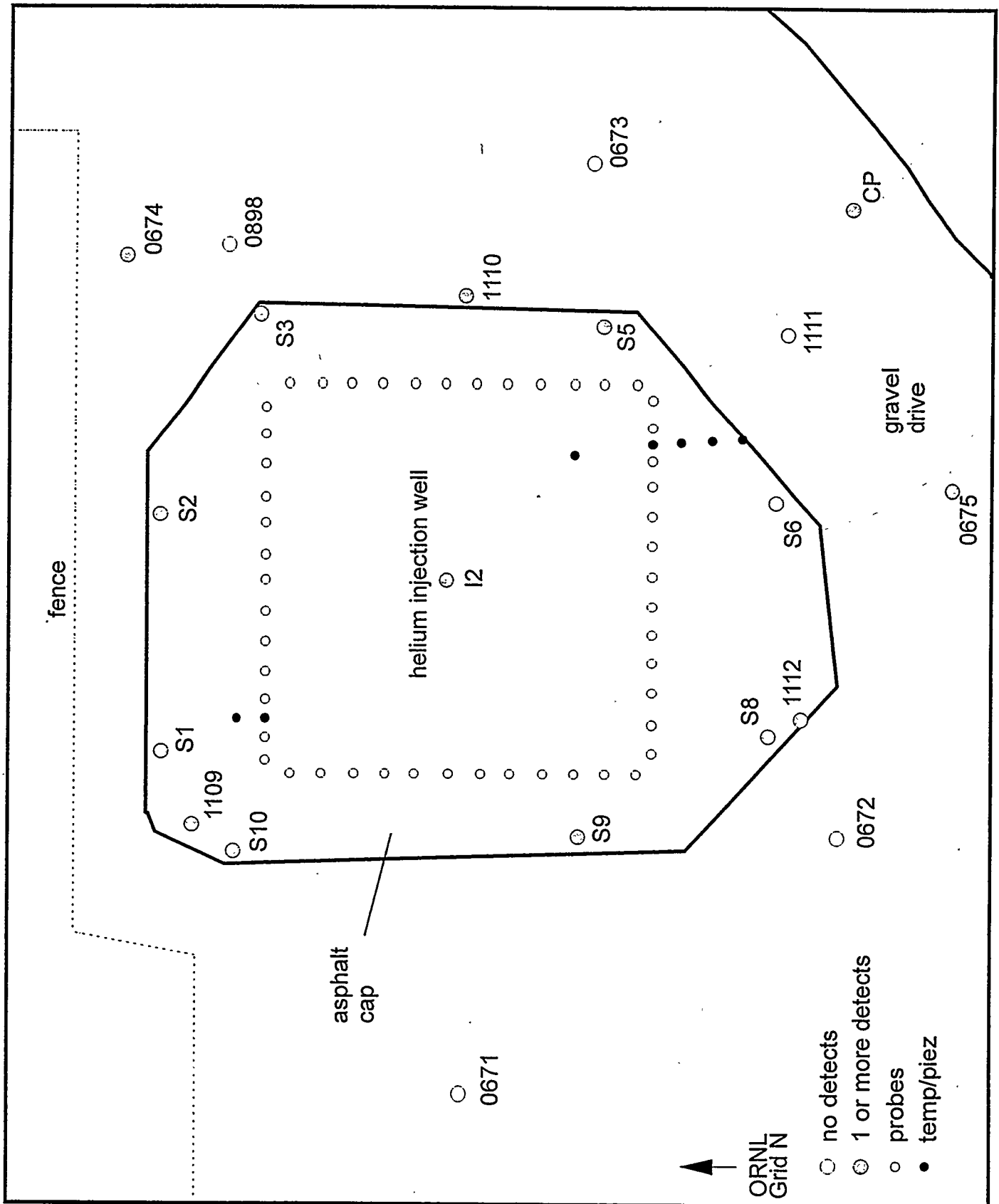


Figure 27. Locations where helium was detected during the tracer injections.

completion at a depth of 32 feet. Auger refusal represents the depth at which the bedrock is substantially less weathered, providing more resistance to the drill bit. However, the transition zone, the interface between highly weathered saprolite and competent bedrock, very likely extends several feet below auger refusal. This zone is an important transport zone on the ORR because it contains a dense network of open fractures. Extension of the probes to 30' should ensure that this layer is bridged by the cryogenic barrier. Sediments were monitored for beta and gamma radiation during augering, and were classified as Category I (≤ 2 mRad/hr), Category II (> 2 mRad/hr), and Category III (> 5 mRad/hr) and disposed of accordingly. Because augered sediments were carried up the auger flights behind the drill bit (ie., the drill bit was deeper than the depth represented by the sediments seen at the surface at any given time), the depths to intervals between the surface and bedrock are only approximate. However, the cross sections are generally consistent with the original pond construction, particularly with respect to the berm which controlled the upper elevation of the original pond. The attached cross sections described below represent an approximate description of the subsurface characteristics and contaminant distribution based on the drill logs and hydrology.

Figure 28 shows the aerial distribution of Category III soils, location of the probe and piezometer boreholes, and key features of the original pond construction. Additional details can be observed in the cross sections identified in Figure 28 and shown in Figure 29. The pond construction information was obtained using the pre-construction engineering drawing [D-19938, R-2, 1955], and therefore the locations of the ditches, berms, and drainage pipes may not reflect the As-Built locations exactly. For example, the actual location of the influent and effluent pipelines may be indicated by the location of conductivity anomalies observed during the electromagnetic survey [Kaufmann, 1996], as shown in Figure 12. These locations are coincident with very high soil radionuclide contamination levels that extend well below the elevation of the berm, lending validity to these locations as regions where the impoundment was penetrated. Later drawings [e.g., Stansfield and Francis, 1986] also indicate that the base of the pond is consistent with the engineering drawing, but that the surface expression of the pond extended beyond the engineering projection at the north and south ends.

The soil contamination patterns indicate two primary locations where the contaminated soils are concentrated: a shallow pathway at or near the elevation of the berm, and deeper pathways that are in all likelihood associated with the location of pipelines into or out of the impoundment. The former could be a result of either overflow of the pond and concentration of contaminants in the soils of the surrounding drainage ditches prior to capping, or subsurface transport through the more permeable fill material above the impoundment walls due the rise in the water table following cap installation. According to Stansfield and Francis [1986], the water table rose several feet higher than when the pond was in operation and higher than was projected in response to cap installation. The deeper contaminant concentrations could have been due to either leakage through the pipes themselves or transport along the soils surrounding the pipes. The existence of higher permeability associated with the contaminant concentrations is supported by the water level data, as discussed in the previous section, as well as the geologic cross sections. The following paragraphs discuss the geologic cross sections and associated

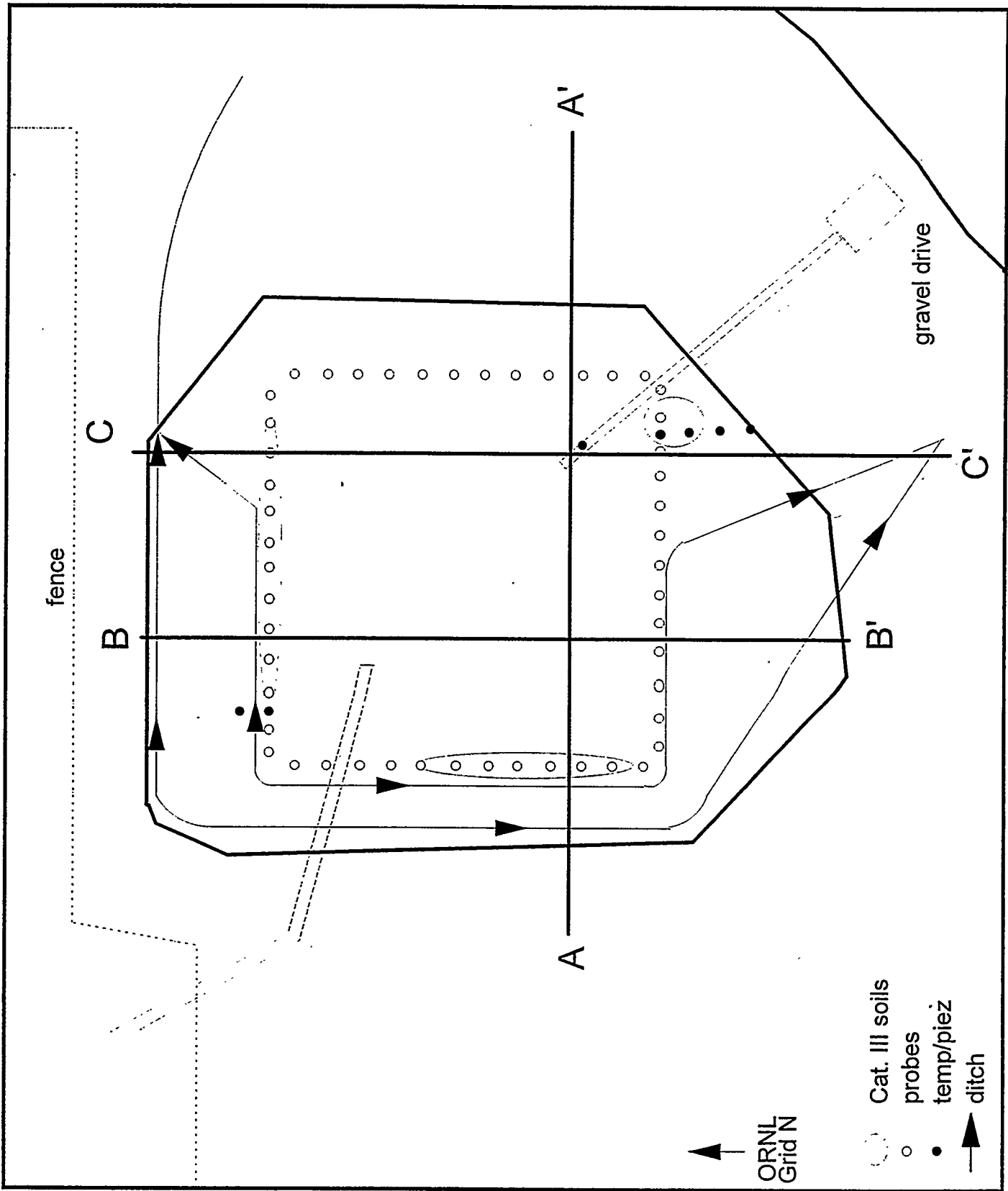


Figure 28. Original impoundment drainage configuration. Cross section locations for fig. 29 are identified.

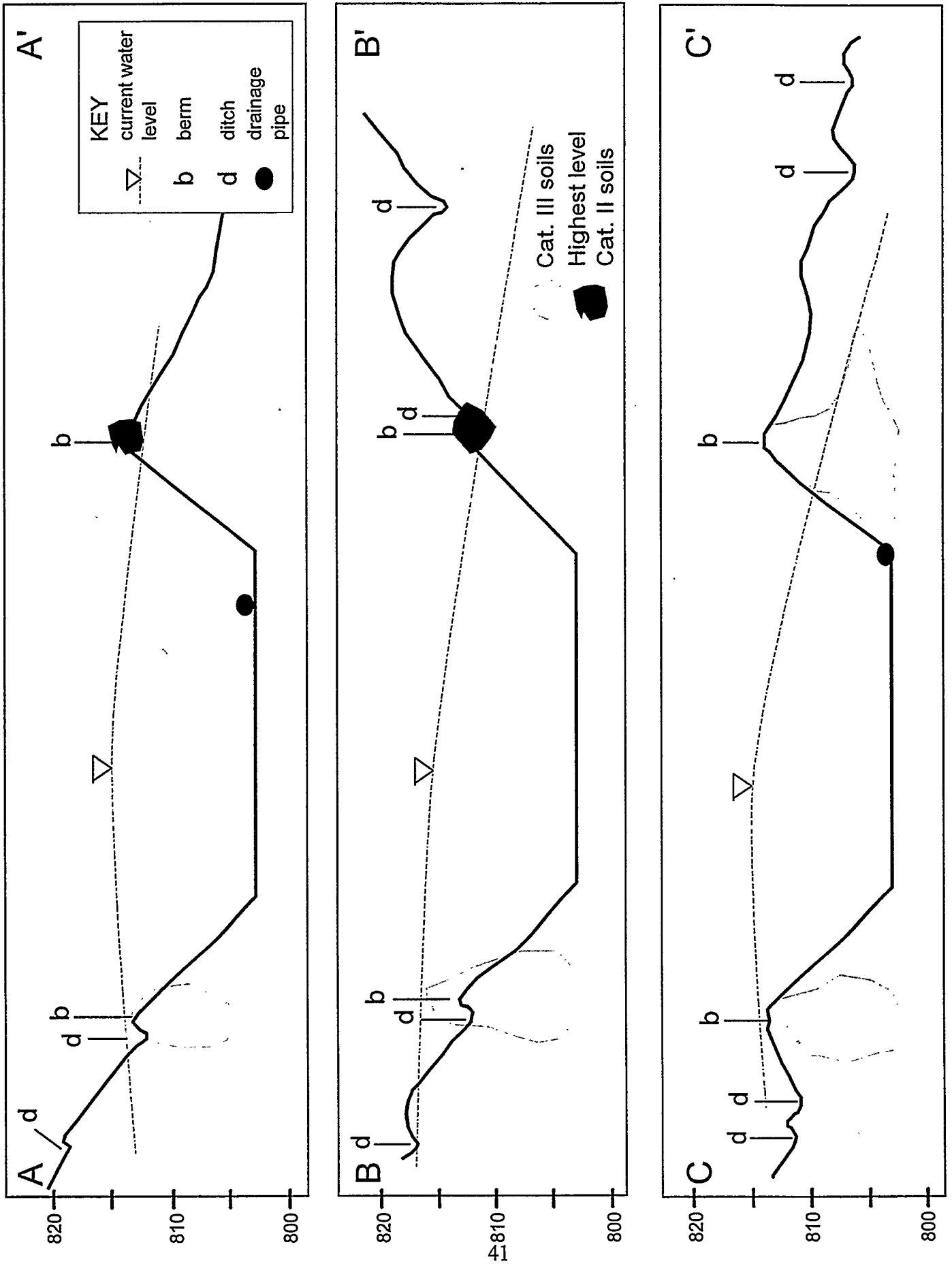


Figure 29. Cross sections of the original impoundment configuration with contaminated soil locations identified.

contaminant transport pathways in greater detail.

4.3. HRE-Pond Geologic Cross Sections

Geologic cross sections were constructed from the information obtained during the drilling of the boreholes for the cryogenic barrier installation. These cross sections contain general descriptions of the materials encountered during drilling, soil contamination data, and the elevation of the original berm surrounding the impoundment. Presumably, the boreholes were drilled directly into the original berm. In all cases, the elevations are approximate and the depth to bedrock represents auger refusal where drilling to refusal occurred.

West Wall (Figure 30)

Coarse gravel was encountered immediately beneath the asphalt cover at every borehole location. This layer extends at least a foot in thickness, and is underlain by a mix of dry soil and gravel fill that becomes increasingly moist and clay-rich. The presence of pieces of decaying wood and subangular pebbles at depth provides further indication that the material is backfill covering the original pond construction. The berm surrounding the original containment pond extends to an elevation of 813' per construction diagrams. At a depth approximately coincident with the elevation of the berm, sticky to wet yellow-brown clay was encountered, which grades to wet soupy saprolite in all but the northern and southern ends, where the clay is underlain by dry saprolite. Depth to bedrock is variable, ranging from 15' at the grid south end to 9.5' at the north end, and is probably controlled by bedrock composition and structure (dip).

Category II soils were encountered in all boreholes, with Category III soils encountered in most. At the southern end, these Cat. III soils are underlain by Cat. II soils, indicating that the highest contamination is concentrated in a relatively narrow interval, coincident with the former berm and/or the top of bedrock. This could have been a result of spillover of the berm when the containment pond was active, or due to preferential flow through the transition zone and in the relatively more permeable fill material above the clay. The clay itself provides significant surface area for sorption of cesium and strontium, and the small pore size could result in retention of contaminant-laden groundwater.

The presence of dry saprolite beneath the clay layer suggests that a perched water table exists at the east side of the impoundment. The water table is located at the approximate depth indicated in Figure 30 based on interpolation between the center stand pipe and other standpipes on the eastern side of the cap as well as the approximate depth to moist sediments logged during drilling.

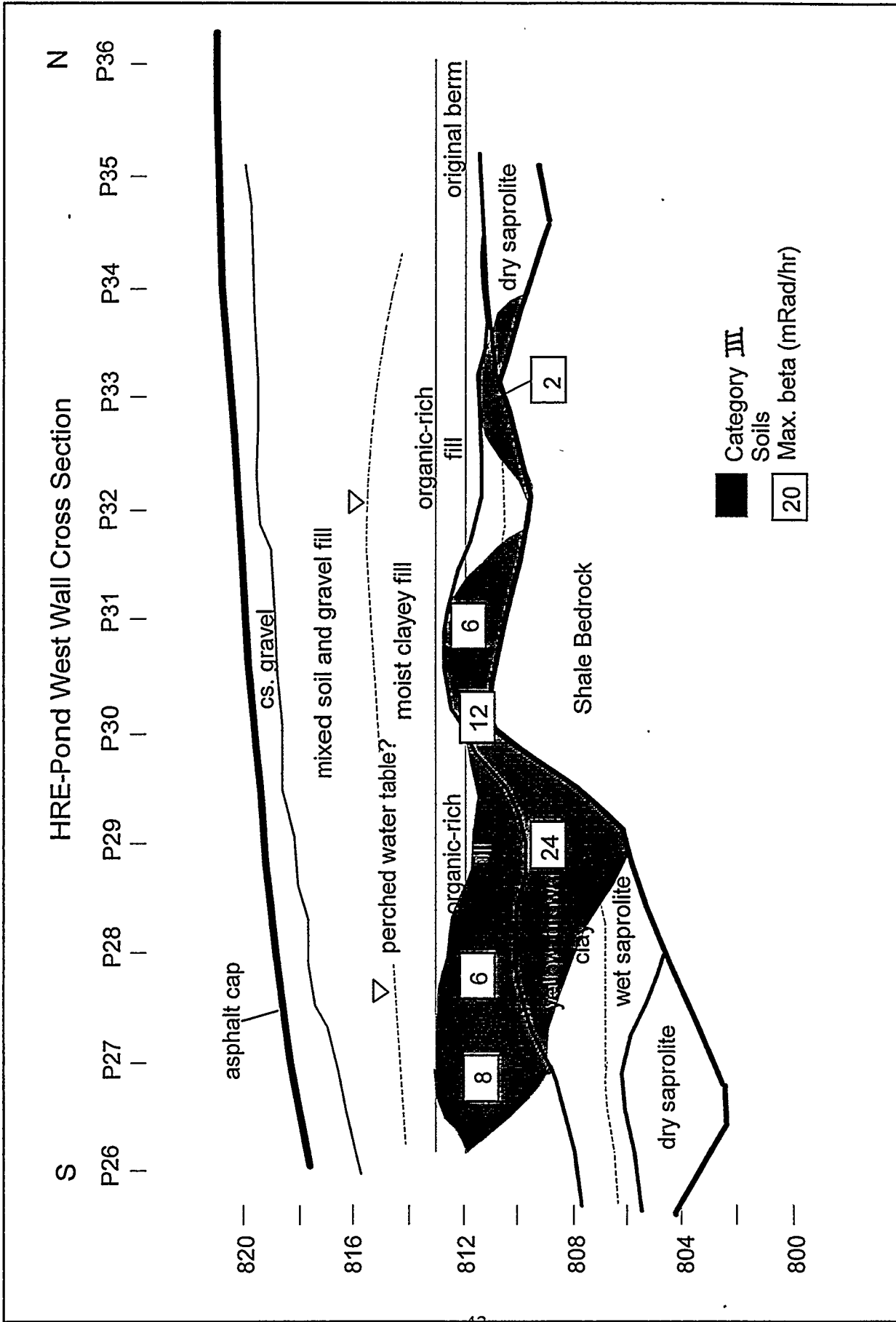


Figure 30. Cross section of the west wall of the impoundment showing gross soil descriptions and approximate location of contaminated soil.

North Wall (Figure 31)

Most of the boreholes along the north wall were not logged during drilling. However, general information was obtained from the drilling crew. Very high levels of soil contamination were encountered in the western half of the section. The highest contamination was associated with wet soils that were described as gun-metal grey with the consistency of masonry cement [Scott Gilbert, Highland Drilling, pers. comm.]. The vertical extent of the contamination in this area is unknown because air-rotary drilling was initiated prior to auger refusal in order to prevent the spread of contaminated soil. This zone is coincident with a conductivity anomaly that was identified during the EM survey extending in a N-S direction and possibly representing a buried pipeline [Kaufman, 1996]. Although this is not the location for the inlet pipeline indicated on the engineering diagram, there are no As-Built diagrams available to confirm the final location of that pipeline. The consistency of the soils suggests that the integrity of the berm has degraded in this location, providing a major pathway for release of contaminants along the north edge of the cap. This could also explain the relatively consistent presence of helium in the wells and standpipes at the NW corner of the pond in spite of their apparent upgradient location.

East Wall (Figure 32)

No Category III soils were detected along the east wall of the impoundment. The original berm was constructed using a dense red clay mixture that was easily identified during drilling. The highest levels of Category II contamination were concentrated in an organic-rich layer no more than 1-ft thick immediately overlying the berm, suggesting shallow transport due to pond overflow prior to burial and/or subsequent transport through less permeable material above the clay subsequent to burial. Well 1110 contains contaminated sediments based on scans of the wipes used during sampling suggesting intersection with a deeper exit pathway, possibly from the base of the pond or even underflowing the pond from an upgradient release point such as the contaminated soils associated with the storage tank previously located just north of the impoundment.

South Wall (Figure 33, 34)

Multiple exit pathways are indicated by the distribution of contaminated soil along the south wall, especially near the SE corner. Category III soils with higher gamma/beta ratio were identified within a narrow band at a location near the planned installation of a drainage pipe in the SE corner of the impoundment and an elevation consistent with base of the pond. The higher contamination is also located near an EM anomaly that was speculated to be buried scrap metal [Kaufman, 1996]. The elevated gamma/beta ratio indicates a higher concentration of ^{137}Cs , which was confirmed to be the major source of gamma radiation [S.Y. Lee, personal comm.]. A N-S cross section along the line of temperature probes (Figure 34) shows that this contamination extends out from the pond to the south as might be expected if the exit pathway were a high-permeability channel such as might have been created by the backfill around the drainage pipe. The water level data from S-6 confirm the presence of conduit-type flow in that vicinity, with very fast flow above the elevation of the bottom of the impoundment.

A second contamination zone is associated with an organic layer overlying the dense red clay of

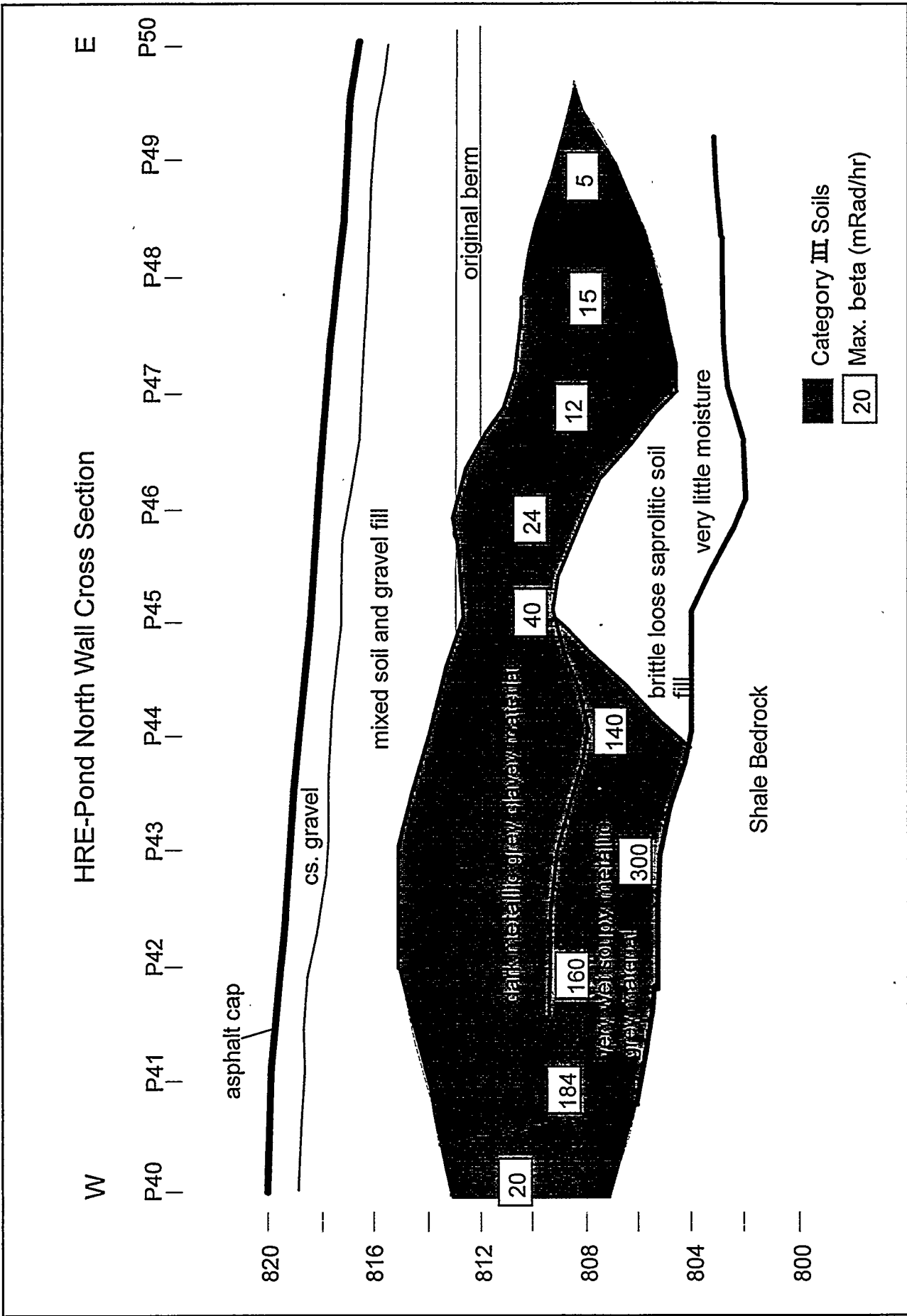


Figure 31. Cross section of the north wall of the impoundment showing gross soil descriptions and approximate location of contaminated soil.

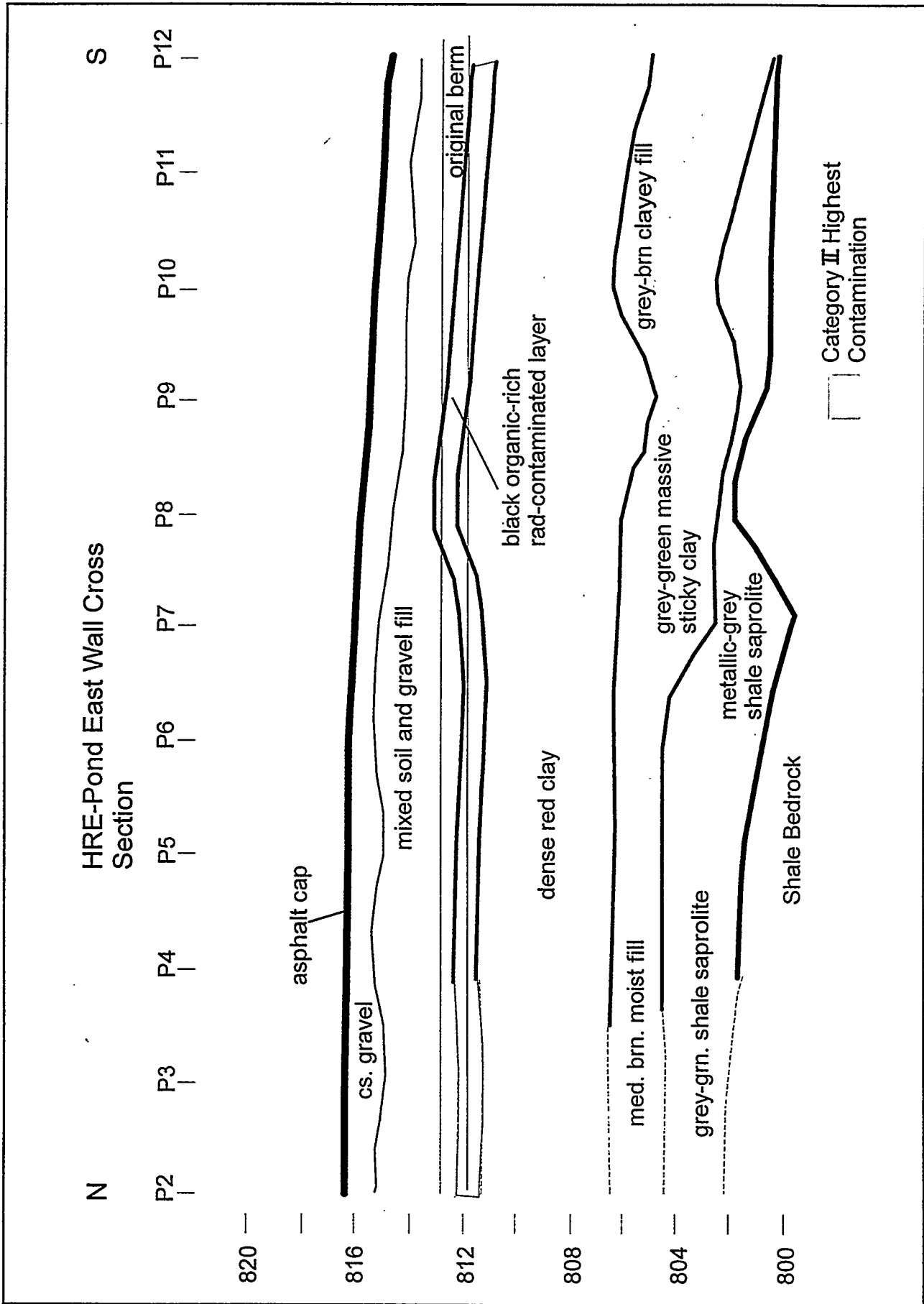


Figure 32. Cross section of the east wall of the impoundment showing gross soil descriptions and approximate location of contaminated soil.

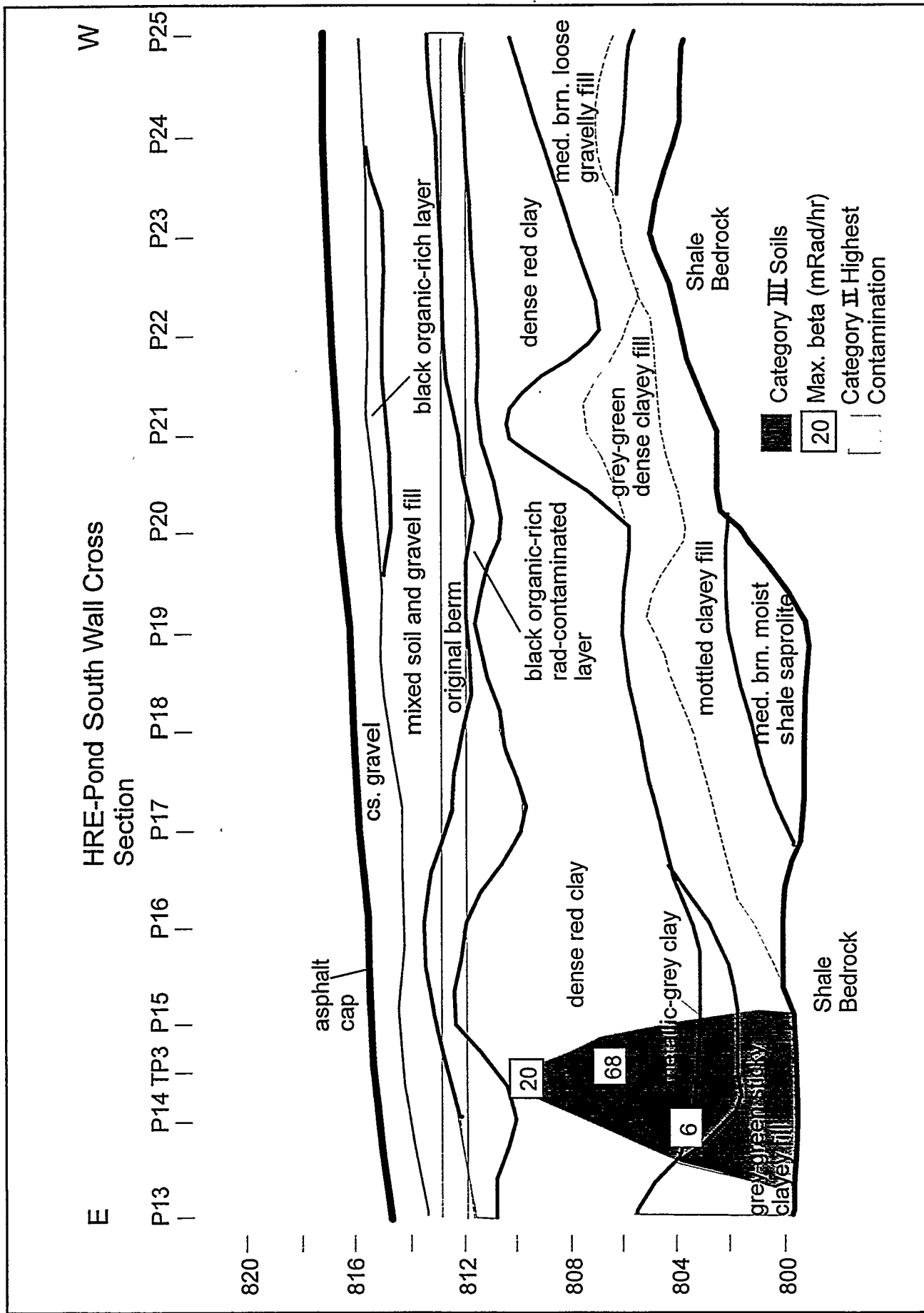


Figure 33. Cross section of the south wall of the impoundment showing gross soil descriptions and approximate location of contaminated soil.

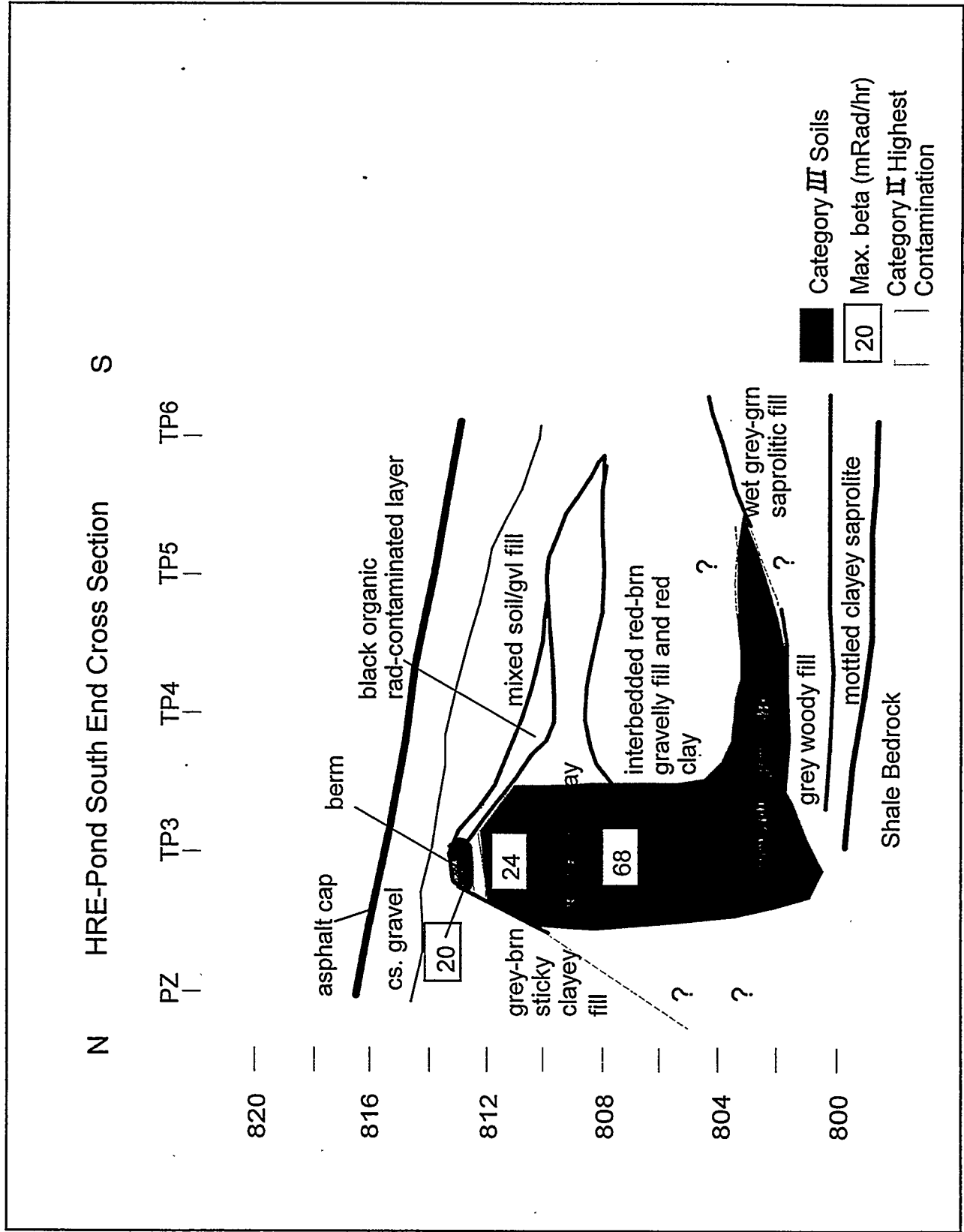


Figure 34. Cross section through the south end of the impoundment showing gross soil descriptions and approximate location of contaminated soil.

the original berm, similar to that observed along the east wall. A third contamination zone is observed at depth in SW corner of the impoundment, associated with a the yellow clay zone just above the bedrock and probably continuous with the zone of contamination observed along the west wall.

5. CONCLUSIONS

5.1. Conclusions

1. *The impoundment is hydrologically active and connected to surrounding soils.* This conclusion is supported by the rapid water level and temperature response to storms, both in and around the pond, by the presence of contaminated soils immediately outside of the impoundment, and by the transport of helium and dye tracers out of the pond.

2. *Contaminant release from the impoundment is probably episodic and correlated to storms.* A rapid and substantial rise in water levels in and around the pond during storm events is evident in all of the well hydrographs. Water level elevations exceed the elevation of the original berm during these events and, in some cases, even intersect the elevation of the gravel layer. High permeabilities in the material overlying the impoundment are evident by the steep slope of the storm recession curves.

3. *Multiple contaminant exit pathways exist that are largely controlled by the nature of the geology within which the impoundment was constructed, the construction design of the impoundment, and the subsequent burial and cap installation.* These potential pathways include 1) transport from the base of the pond through the highly fractured shallow bedrock, possibly enhanced by the sand-filled boreholes that provide vertical pathways through the pond sediments, and through the fill around the effluent pipeline; 2) transport through the more permeable fill materials overlying the original impoundment; 3) transport through the gravel layer immediately below the asphalt cap; and 4) transport through the walls of the original impoundment, possibly related to influent/effluent pipelines and fractures in the walls of the pond.

4. *Differences in transport of the dye and gas tracers is most likely due to flooding the impoundment for several days following dye injection.* It is clear that the dye tracer was transported in many directions under artificially-induced gradients. However, the helium tracer test demonstrated that transport out of the pond occurs under ambient conditions as well, and that release from the impoundment is greatest during the winter wet months, probably as a result of higher overall water levels and more frequent high-intensity storms. Further, the helium tracer test demonstrated transport in the NW corner, contrary to expectations but consistent with the distribution of contaminated soils.

5.2. Recommendations

1. *Post-barrier tracer tests using bromide and a continuous injection method similar to that used at WAG 5 [Knowles et al., 1995].* The use of a continuous bromide injection has several

advantages over other tracer methods. Continuous injection allows sufficient mass to be introduced over time, avoids artificially raising the water table in the pond, and avoids density effects. Bromide is inexpensive, non-sorbing, can be easily analyzed with ion chromatography methods for sensitive detection, and circumvents any uncertainty associated with previous dye injections at this and surrounding sites. Finally, the method provides a means for measuring the groundwater flux through the injection well.

2. *Sampling strategies for monitoring releases from the impoundment must take episodic transport into account.* Sampling for tracers and/or radionuclides must be conducted frequently enough and timed relative to storm events to capture any episodic transport behavior. Infrequent monitoring at pre-determined intervals may miss the transport of tracers unless sufficient mass is injected and sufficient time allowed to achieve consistent breakthrough.

3. *Continued water level and temperature monitoring throughout FY98.* Water level and temperature monitoring should be continued during and following the installation of the cryo-barrier in order to determine changes in subsurface hydrology related to barrier installation. Temperature monitoring can provide an indication of heat flux in the area surrounding the barrier. Continued monitoring through the year can be used to determine the impact of seasonal variations on barrier integrity.

ACKNOWLEDGEMENTS

Support for this project was provided by DOE/Office of Technology Development (EM-50). Field efforts were greatly assisted by Jeff Riggs and Roy Freeman of the ORNL Instruments and Controls Division. Drew Diefendorf, Dale Huff, and Craig Rightmire of the ORNL Environmental Sciences Division provided helpful review and comments.

6. REFERENCES CITED

- Field, M.S., 1996. Final Report on the Initial Ground-Water Tracing Results for the Freeze-Barrier Demonstration. U.S. EPA SITE Program, October 31, 1996.
- Hatcher, R.D., Jr., P.J. Lemiszki, R.B. Dreier, R.H. Ketelle, R.R. Lee, D.A. Leitzke, W.M. McMaster, J.L. Foreman, and S.Y. Lee, 1992. Status Report on the Geology of the Oak Ridge Reservation. ORNL/TM-12074.
- Huff, D.D., and W.E. Sanford, 1985. The use of tracers to confirm sources for radioactively contaminated seeps. EOS, Transactions of the American Geophysical Union, v. 76(4) supplement, p.F245.
- Jardine, P.M., W.E. Sanford, O.C. Reedy, and J.P. Gwo, 1995. Multicomponent tracer injection at a DOE waste disposal site with fractured porous media: II. Experimental findings. EOS, Transactions of the American Geophysical Union, v. 76(4) supplement, p.F251.
- Kaufman, R., 1996. Electromagnetic conductivity survey of the HRE Pond, memo to Mike Harper, LMES, April 8, 1996.
- Knowles, T.L., J.F. McCarthy, and W.E. Sanford, 1995. Multiple nonreactive and reactive tracers to investigate the migration of transuranics in groundwater. EOS, Transactions of the American Geophysical Union, v. 76(4) supplement, p.F238.
- Moline, G.R., and M.E. Schreiber, 1996. FY94 Site Characterization and Multilevel Well Installation at a West Bear Creek Valley Research Site on the Oak Ridge Reservation. ORNL/TM-13029.
- Moline, G.R., 1996. Status Report: HRE-Pond Cryogenic Barrier Demonstration Noble Gas Tracer Test. Internal project report, September 19, 1996.
- Sanford, W.E., Shropshire, R.G., and D.K. Solomon, 1996. Dissolved gas tracers in groundwater: Simplified injection, sampling, and analysis. Water Resources Research, v. 32 (6), p.1635-1642.
- Shevenell, 1996. Analysis of well hydrographs in a karst aquifer: estimates of specific yields and contrinuum transmissivities. Journal of Hydrology, v.174(1996), p.331-355.
- Stansfield, R.G., and C.W. Francis, 1986. Characterization of the Homogeneous Reactor Experiment No. 2 (HRE) Impoundment. ORNL/TM-10002.